Economic natural resource deposits at terrestrial impact structures

Richard A. F. Grieve

Geological Society, London, Special Publications 2005; v. 248; p. 1-29
doi:10.1144/GSL.SP.2005.248.01.01

Economic natural resource deposits at terrestrial impact structures

RICHARD A. F. GRIEVE
Earth Sciences Sector, Natural Resources Canada, Ottawa, Ontario, Canada K14 0E4

Abstract: Economic deposits associated with terrestrial impact structures range from world-class to relatively localized occurrences. The more significant deposits are introduced under the classification: progenetic, syngenetic or epigenetic, with respect to the impact event. However, there is increasing evidence that post-impact hydrothermal systems at large impact structures have remobilized some progenetic deposits, such as some of the Witwatersrand gold deposits at the Vredefort impact structure. Impact-related hydrothermal activity may also have had a significant role in the formation of ores at such syngenetic 'magmatic' deposits as the Cu–Ni–platinum-group elements ores associated with the Sudbury impact structure. Although Vredefort and Sudbury contain world-class mineral deposits, in economic terms hydrocarbon production dominates natural resource deposits found at impact structures. The total value of impact-related resources in North America is estimated at US$18 billion per year. Many impact structures remain to be discovered and, as targets for resource exploration, their relatively invariant, but scale-dependent properties, may provide an aid to exploration strategies.

Natural impact craters are the result of the hypervelocity impact of an asteroid or comet with a planetary surface and involve the virtually instantaneous transfer of the considerable kinetic energy in the impacting body to a spatially limited, near-surface volume of a planet's surface. Impact is an extraordinary geological process involving vast amounts of energy, and extreme strain rates, causing immediate rises in temperature and pressure that produce fracturing, disruption and structural redistribution of target materials. This is followed by a longer period of time during which the target rocks readjust to the 'local' structural and lithological anomaly that constitutes the resultant impact structure and re-equilibrate from the thermal anomaly that is the result of shock metamorphism. Currently, around 170 individual terrestrial impact structures or small crater fields have been recognized, with the discovery rate of around five new structures per year. A listing of known terrestrial impact structures and some of their salient characteristics (location, size, age, etc.) is maintained by the Planetary and Space Science Centre at the University of New Brunswick and can be found at: http://www.unb.ca/passc/ImpactDatabase/index.html

Some economic deposits of natural resources occur within specific impact structures or are, in someway, impact-related. Masaitis (1989, 1992) noted approximately 35 known terrestrial impact structures that have some form of potentially economic natural resource deposits. In a review of the economic potential of terrestrial impact structures, Grieve & Masaitis (1994) reported that there were 17 known impact structures that have produced some form of economic resources. This contribution represents an update of their review. In the intervening 10 years, there has been clarification of both the nature and relation of the resource to the specific impact event and a greater understanding of impact processes and the character of specific impact structures. As with Grieve & Masaitis (1994), this contribution is not comprehensive with respect to all natural resources related to terrestrial impact structures and does not consider those structures that have been or are being exploited as a source of aggregate, lime or stone for building material (e.g. Ries, Rouchechouart), are a source of groundwater or serve as reservoirs for hydroelectric power generation (e.g. Manicouagan, Puchezh-Katunki). However, the economic worth of these types of natural resources at terrestrial impact structures can be considerable. For example, the hydroelectric power generated by the Manicouagon reservoir is of the order of 4500 GWh per year, sufficient to supply power to a small city and worth approximately US$200 million per year.

The examples considered here are the resource deposits directly related to the impact structure, through structural disturbance and/or brecciation of the target rocks, impact heating and/or hydrothermal activity, and the formation of a structural or topographic trap. This contribution follows the logic and the terminology of Grieve & Masaitis (1994); namely, deposits are considered in the order progenetic, syngenetic, epigenetic. The most significant development in

From: McDonald, I., Boyce, A. J., Butler, I. B., Herrington, R. J. & Polya, D. A. (eds) 2005. *Mineral Deposits and Earth Evolution*. Geological Society, London, Special Publications, **248**, 1–29. 0305-8719/$15.00

viewing natural resources deposits at terrestrial impact structures, since Grieve & Masaitis (1994), is the recognition of a greater role for impact-related, post-impact hydrothermal activity in impact events (e.g. McCarville & Crossey 1996; Ames *et al.* 1998, 2005; Osinski *et al.* 2001; Naumov 2002). The remobilization of progenetic deposits has blurred some of the separation between progenetic and syngenetic deposits, and hydrothermal deposits are considered as a continuation of syngenetic processes, not as epigenetic as in Grieve & Masaitis (1994).

Characteristics of terrestrial impact structures

Morphology

On most planetary bodies, impact structures are recognized by their characteristic morphology and morphometry. Detailed appearance, however, varies with crater diameter. With increasing diameter, impact structures become proportionately shallower and develop more complicated rims and floors, including the appearance of central peaks and interior rings. Impact craters are divided into three basic morphologic subdivisions: simple craters, complex craters, and basins (Dence 1972; Wood & Head 1976).

Simple impact structures have the form of a bowl-shaped depression with an upraised rim (Fig. 1). At the rim, there is an overturned flap of ejected target materials, which displays inverted stratigraphy, with respect to the original target materials. Beneath the floor is a lens of brecciated target material that is roughly parabolic in cross-section. This breccia lens consists of allochthonous material. In places, the breccia lens may contain highly shocked (even melted) target materials. Beneath the breccia lens, parautochthonous, fractured rocks define the walls and floor of what is known as the true crater. Shocked rocks in the parautochthonous materials of the true crater floor are confined to a small central volume at the base.

With increasing diameter, simple craters display increasing evidence of wall and rim collapse and evolve into complex craters. Complex impact structures on Earth are found with diameters greater than 2 km in layered, sedimentary target rocks but not until diameters of 4 km or greater in stronger, more homogeneous, igneous or metamorphic, crystalline target rocks (Dence 1972). Complex impact structures are characterized by a central topographic peak or peaks, a broad, flat floor, and

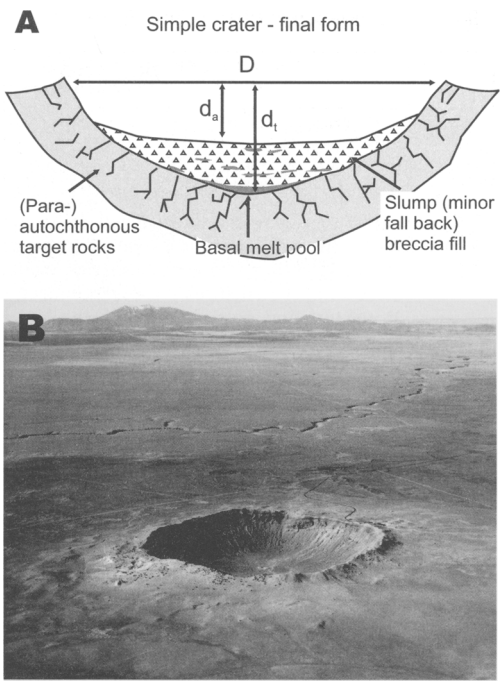

Fig. 1. (**A**) Schematic cross-section of a terrestrial simple impact structure. No vertical exaggeration. D is diameter and d_a and d_t are apparent and true depth, respectively. (**B**) Oblique aerial photograph of the 1.2 km diameter terrestrial simple impact structure, Barringer, Arizona, USA.

terraced, inwardly slumped and structurally complex rim areas (Fig. 2). The broad flat floor is partially filled by a sheet of impact melt rock and/or polymict allochthonous breccia. The central region is structurally complex and, in large part, occupied by a central peak, which is the topographic manifestation of a much broader and extensive area of structurally uplifted rocks that occurs beneath the centre of complex craters. Grieve & Therriault (2004) and Melosh (1989), respectively, provide further details of observations of terrestrial crater forms and cratering mechanics at simple and complex structures.

There have been claims that the largest known terrestrial impact structures have multi-ring forms, e.g. Chicxulub (Sharpton *et al.* 1993), Sudbury, Canada (Stöffler *et al.* 1994; Spray & Thompson 1995), and Vredefort (Therriault *et al.* 1997). Although some of their geological and geophysical attributes form annuli, it is not clear whether these correspond, or are related in origin, to the obvious topographical rings observed in lunar multi-ring basins (Spudis

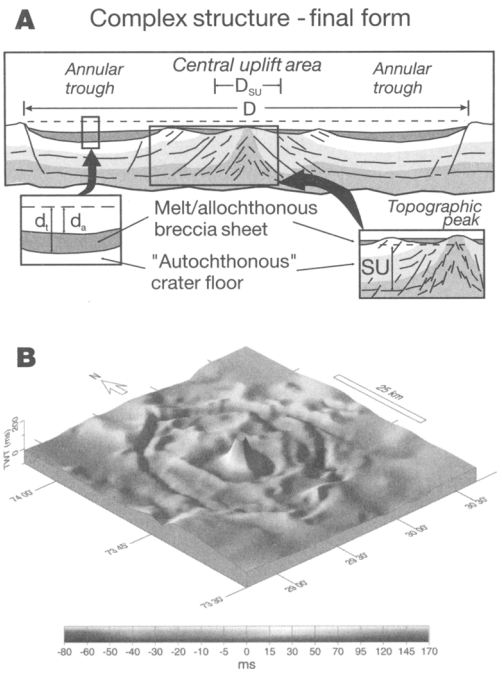

Fig. 2. (**A**) Schematic cross-section of a terrestrial complex impact structure. No vertical exaggeration. Abbreviations are as in Fig. 1, with SU as the vertical amount of structural uplift, and D_{su} as the diameter of the structural uplift, at its base. (**B**) 3D topography of a relatively uneroded complex impact structure, with a central peak and a possible peak ring, as illustrated by the residual two-way travel time just above the impact horizon at the Mjølnir impact structure, in the Barents Sea. View is from the SW, at an angle of 30° above the horizon. Note top of central peak has been eroded off. Vertical exaggeration is 20 times. Source: F. Tsikalas, University of Oslo.

1993; Grieve & Therriault 2000). Attempts to define morphometric relations, particularly depth–diameter relations, for terrestrial impact structures have had limited success, because of the effects of erosion and, to a lesser degree, sedimentation. The most recent empirical relations can be found in Grieve & Therriault (2004).

Geology of impact structures

Although an anomalous circular topographic, structural, or geological feature may indicate the presence of an impact structure on Earth, there are other geological processes that can produce similar features in the terrestrial environment. The burden of proof for an impact origin in the terrestrial environment for a particular structure or lithology in the stratigraphic record generally lies with the documentation of the occurrence of shock-metamorphic effects.

On impact, the bulk of the impacting body's kinetic energy is transferred to the target by means of a shock wave. This shock wave imparts kinetic energy to the target, which leads to the formation of a crater and the ejection of target materials. It also increases the internal energy of the target materials, which leads to the formation of so-called shock-metamorphic effects. Details of the physics of shock wave behaviour and shock metamorphism can be found in Melosh (1989) and Langenhorst (2002). Shock metamorphism is the progressive breakdown in the structural order of minerals and rocks and requires pressures and temperatures well above the pressure–temperature field of endogenic terrestrial metamorphism (Fig. 3). Minimum shock pressures required for the production of diagnostic shock-metamorphic effects are 5–10 GPa for most silicate minerals. Strain rates produced on impact are of the order of 10^6 s^{-1} to 10^9 s^{-1} (Stöffler & Langenhorst 1994), many orders of magnitude higher than typical tectonic strain rates (10^{-12} s^{-1} to 10^{-15} s^{-1}; e.g. Twiss & Moores 1992), and shock-pressure duration is measured in seconds, or less, in even the largest impact events (Melosh 1989). Endogenic geological processes do not reproduce these physical conditions. They are unique to impact and, unlike endogenic terrestrial metamorphism, disequilibrium and metastability are common phenomena in shock metamorphism. Shock-metamorphic effects are well described in papers by Stöffler (1971, 1972, 1974), Stöffler

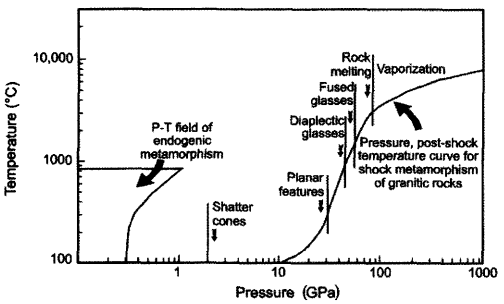

Fig. 3. Logarithmic plot of shock pressure (GPa) against post-shock temperature (°C) range of shock metamorphism for granitic rocks, with pressure ranges of some specific shock metamorphic effects indicated. Shown for comparison is the pressure–temperature range of endogenic terrestrial metamorphism.

& Langenhorst (1994), Grieve *et al.* (1996), French (1998), Langenhorst & Deutsch (1994), Langenhorst (2002) and others. They are discussed here only in general terms, as they relate to the recognition of impact materials in the terrestrial environment.

Impact melting. During shock compression, there is considerable pressure–volume work but pressure release occurs adiabatically. Heating of the target rocks occurs, as not all the pressure–volume work is recovered upon pressure release and the excess is manifest as irreversible waste heat. Above 60 GPa, the waste heat is sufficient to cause whole-rock melting and, at higher pressures, vaporization (Melosh 1989). Impact melted lithologies occur as glass particles and bombs in crater ejecta (Engelhardt 1990), as dykes within the crater floor and walls, as glassy to crystalline pools and lenses within the breccia lenses of simple craters, or as coherent, central sheets lining the floor of complex structures (Fig. 4).

The final composition of impact-melt rocks depends on the wholesale melting of a mix of target rocks, in contrast to partial melting and/or fractional crystallization relationships that occurs in endogenous igneous rocks. The composition of impact-melt rocks is, therefore, characteristic of the target rocks and may be reproduced by a mixture of the various country rock types in their appropriate geological proportions. Such parameters at $^{87}Sr/^{86}Sr$ and $^{143}Nd/^{144}Nd$ ratios of impact-melt rock also reflect the pre-existing target rocks (Jahn *et al.* 1978; Faggart *et al.* 1985). In general, even relatively thick impact-melt sheets are chemically homogeneous over radial distances of kilometres. In large impact structures, and where the target rocks are not homogeneously distributed, this observation may not hold true in detail, such as for Manicougan, Canada (Grieve & Floran 1978), Chicxulub (Kettrup *et al.* 2000), and Popigai (Kettrup *et al.* 2003). Differentiation is not a characteristic of relatively thick coherent impact-melt sheets, with the exception of the extremely thick *c.* 2.5 km, Sudbury Igneous Complex, Sudbury Structure, Canada (Ariskin *et al.* 1999; Therriault *et al.* 2002).

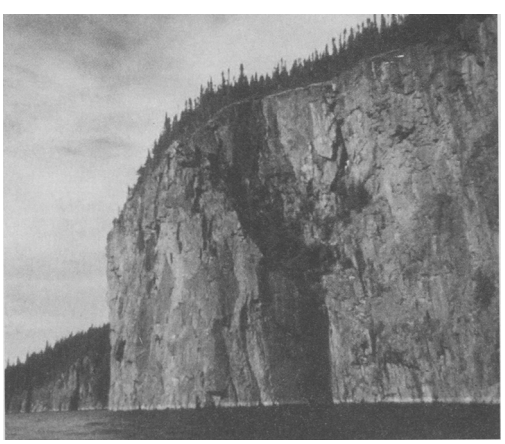

Fig. 4. Approximately 150 m high cliffs of impact melt rock at the edge of the inner plateau at Manicouagan impact structure.

Enrichments above target rock levels in siderophile and platinum-group elements (PGE) and Cr have been identified in some impact-melt rocks and ejecta. These are due to an admixture of up to a few percent of meteoritic material from the impacting body. In some melt rocks, the relative abundances of the various siderophiles have constrained the composition of the impacting body to the level of meteorite class (Palme *et al.* 1979; McDonald *et al.* 2001). In other melt rocks, no geochemical anomaly has been identified. This may be due to the inhomogeneous distribution of meteoritic material within the impact-melt rocks and sampling variations (Palme *et al.* 1981), or to differentiated impacting bodies, such as basaltic achondrites. More recently, high precision Cr, Os and He-isotopic analyses have been used to detect meteoritic material in the terrestrial environment (e.g. Koeberl *et al.* 1994; Koeberl & Shirley 1997; Peucker-Ehrenbrink 2001; Farley 2001).

Fused glasses and diapletic glasses. Shock-fused minerals are characterized morphologically by flow structures and vesiculation. Peak pressures required for shock melting of single crystals are in the order of 40–60 GPa (Stöffler 1972, 1974). Under these conditions, the minerals in the rock melt independently and selectively after the passage of the shock wave. Conversion of framework silicates to isotropic, dense, glassy, but not fused, phases occurs at peak pressures and temperatures, well below their normal melting point. These 'diaplectic glasses' require peak pressures of 30–45 GPa for feldspar and 35–50 GPa for quartz in quartzo-feldspathic rocks (e.g. Stöffler & Hornemann 1972; Stöffler 1984). Diaplectic glass has the same morphology as the original mineral crystal (Fig. 5), and a lower density than the crystalline form from which it is derived (but higher than thermally melted glasses of equivalent composition; e.g. Stöffler & Hornemann 1972; Langenhorst & Deutsch 1994).

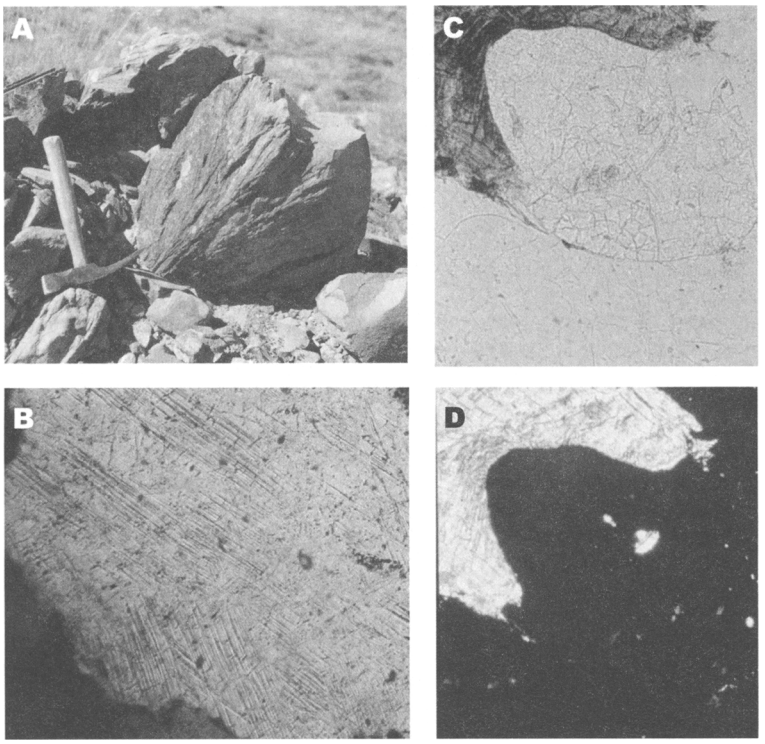

Fig. 5. Some shock metamorphic effects. (**A**) Shatter cones at Gosses Bluff impact structure. (**B**) Photomicrograph of planar deformation features (PDFs) in quartz in compact sandstone from Gosses Bluff impact structure. Crossed polars, width of field of view 0.4 mm. (**C**) Photomicrograph of quartz (centre, higher relief) with biotite (darker grey, upper right) and feldspar (white, bottom) in a shocked granitic rock from Mistastin impact structure. Plane light, width of field of view 1.0 mm. (**D**) Photomicrograph as in (c) but with crossed polars. The biotite is still birefringent but the quartz and feldspar are isotropic, as they have been metamorphosed to diaplectic glasses by the shock wave, although retaining their original crystalline shapes.

High-pressure polymorphs. Shock can result in the formation of metastable polymorphs, such as stishovite and coesite from quartz (Chao *et al.* 1962; Langenhorst 2002) and cubic and hexagonal diamond from graphite (Masaitis 1993; Langehorst 2002). Coesite and diamond are also products of high-grade metamorphism but the paragenesis and, more importantly, the geological setting are completely different from those of impact events. The high-pressure polymorphs of quartz (i.e. stishovite and coesite) have only rarely been produced by laboratory shock-recovery experiments (cf. Stöffler & Langenhorst 1994). In terrestrial impact structures in crystalline targets, these polymorphs generally occur in small or trace amounts as very fine-grained aggregates and are formed by partial transformation of the host quartz. In porous quartz-rich target lithologies, however, they may be more abundant. For example, coesite may constitute 35% of the mass of highly shocked Coconino sandstone at Barringer (Kieffer 1971). Further details on the characteristics of coesite and stishovite are given by Stöffler & Langenhorst (1994).

Planar microstructures. The most common documented shock-metamorphic effect is the occurrence of planar microstructures in tectosilicates, particularly quartz (Fig. 5; Hörz 1968). The utility of planar microstructures in quartz reflect the ubiquitous nature of the mineral and the stability of the quartz and microstructures themselves, in the terrestrial environment, and the relative ease with which the microstructures can be documented. Recent reviews of the shock metamorphism of quartz, with an emphasis on the nature and origin of planar microstructures in experimental and natural impacts, are given in Stöffler & Langenhorst (1994), Grieve *et al.* (1996), and Langenhorst (2002). Planar deformation features (PDFs) in

minerals are produced under pressures of *c.* 10–35 GPa. Planar fractures (PFs) form under shock pressures ranging from *c.* 5–35 GPa (Stöffler 1972; Stöffler & Langenhorst 1994).

Shatter cones. The only known large-scale diagnostic shock effect is the occurrence of shatter cones (Dietz 1968). Shatter cones are unusual, striated, and horse-tailed conical fractures (Fig. 5), ranging from millimetres to metres in length, produced by the passage of a shock wave through rocks (e.g. Sagy *et al.* 2002). Shatter cones have been initiated most commonly in rocks that experienced moderately low shock pressures, 2–6 GPa, but have been observed in rocks that experienced *c.* 25 GPa (Milton 1977). These conical striated fracture surfaces are best developed in fine-grained, structrually isotropic lithologies, such as carbonates and quartzites. Generally, they are found as individual or composite groups of partial to complete cones in rocks below the crater floor, especially in the central uplifts of complex impact structures, and rarely in isolated rock fragments in breccia units, indicating the shatter cones formed before the material was set in motion by the cratering flow-field.

Geophysics of impact structures

Geophysical anomalies over terrestrial impact structures vary in their character and, in isolation, do not provide definitive evidence for an impact origin. Interpretation of a single geophysical data set over a suspected impact structure may be ambiguous (e.g. Hildebrand *et al.* 1991; Sharpton *et al.* 1993). However, when combined with complementary geophysical methods and the existing database of other known impact structures, a more definite assessment can be made (e.g. Ormö *et al.* 1999). Since potential-field data are available over large areas, with almost continuous coverage, gravity and magnetic observations have been the primary geophysical indicators used for evaluating the occurrence of possible terrestrial impact structures. Reflection seismic data, although providing much better spatial resolution of subsurface structure (e.g. Morgan *et al.* 2002*a*) are used less often, because datasets are generally less widely available. Electrical methods have been used even less commonly (e.g. Henkel 1992). Given the lack of specificity of the geophysical attributes of terrestrial impact craters, they are not discussed here. The most recent synthesis of the geophysical character of terrestrial impact structures is Grieve & Pilkington (1996).

Characteristics of natural resource deposits

The location and origin of economic natural resource deposits in impact structures are controlled by several factors related to the impact process and the specific nature of the target. The types of deposits are classified according to their time of formation relative to the impact event: progenetic, syngenetic and epigenetic (Table 1). Progenetic economic deposits are those that originated prior to the impact event by purely terrestrial concentration mechanisms. The impact event caused spatial redistribution of these deposits and, in some cases, brought them to a surface or near-surface position, from where they can be exploited. Syngenetic deposits are those that originated during the impact event, or immediately afterwards, as a direct result of impact processes. They owe their origin to energy deposition from the impact event in the local environment, resulting in phase changes and melting. Hydrothermal deposits, where the heat source

Table 1. *Genetic groups of natural resource deposits at terrestrial impact structures*

Genetic group	Principal mode of origin	Types of known deposits
Progenetic	Brecciation	Building stone, silica
	Structural displacement	Iron, uranium, gold
Syngenetic	Phase transitions	Impact diamond
	Crustal melting	Cu, Ni, PGE, glass
	Hydrothermal activity	Lead, zinc, uranium, pyrite, gold, zeolite, agate
Epigenetic	Sedimentation	Placer diamond and tektites
	Chemical and biochemical sedimentation	Zeolite, bentonite, evaporites, oil shale, diatomite, lignite, amber, calcium phosphate
	Fluid flow	Oil, natural gas, fresh and mineralized water

was a direct result of the impact event, are also considered to be syngenetic. This differs from Grieve & Masaitis (1994). Epigenetic deposits result from the formation of an enclosed topographic basin, with restricted sedimentation, or the long-term flow of fluids into structural traps formed by the impact structure.

Progenetic deposits

Progenetic economic deposits in impact structures craters include iron, uranium, gold and others (Tables 1 & 2). In many cases, the deposits are relatively small. Only the larger and more active deposits are considered here.

Table 2. *Deposits and/or indications of natural resources in terrestrial impact structures*

Structure	Location (lat.; long.)	Diameter (km)	Economic material	Genetic type of economic deposit
*Ames, USA	36°15′N; 98°10′W	16	Oil, gas	Epigenetic
*Avak, USA	71°15′N; 156°38′W	12	Gas	Epigenetic
*Barringer, USA	35°02′N; 111°01′W	1.2	Earth silica	Progenetic
Beyenchime-Salaatin, Russia	71°50′N; 123°30′W	8	Pyrite	Epigenetic
*Calvin, USA	41°45′N; 85°57′	8.5	Oil	Epigenetic
Boltysh, Ukraine	48°45′N; 32°10′W	24	Oil shale	Epigenetic
*Carswell, Canada	58°27′N; 109°30′W	39	Uranium	Progenetic/ Syngenetic
*Charlevoix, Canada	47°32′N; 70°18′W	54	Ilmenite	Progenetic
*Chicxulub, Mexico	21°20′N; 89°30′W	180	Oil, gas	Epigenetic
*Crooked Creek, USA	37°50′N; 91°23′W	7	Lead, zinc	Syngenetic
Decaturville, USA	37°54′N; 92°43′W	6	Lead, zinc	Syngenetic
Ilyinets, Ukraine	49°06′N; 29°12′E	4.5	Agate	Epigenetic
Kaluga, Russia	54°30′N; 36°15′W	15	Mineral water	Epigenetic
Kara, Russia	69°05′N; 64°18′E	65	Diamond, zinc	Syngentic
Logoisk, Belarus	54°12′N; 27°48′E	17	Amber, calcium phosphate	Epigenetic
*Lonar, India	19°59′N; 76°31′E	1.8	Various salts	Epigenetic
*Marquez, USA	31°17′N; 96°18′W	22	Oil, gas	Epigenetic
Morokweng, S. Africa	26°28′S; 23°32′E	80	Ni-oxides, sulphides, silicates	Syngenetic
Obolon, Ukraine	49°30′N; 32°55′E	15	Oil shale	Epigenetic
Popigai, Russia	71°30′N; 111°00′E	100	Diamond	Syngenetic
Puchezh-Katunki, Russia	57°00′N; 43°35′E	80	Diamond, zeolite	Syngenetic
Ragozinka, Russia	58°18′N; 62°00′E	9	Diatomite	Epigenetic
*Red Wing, USA	47°36′N; 103°33′W	9	Oil, gas	Epigenetic
*Ries, Germany	48°53′N; 10°37′E	24	Diamond, lignite, bentonite, moldavites	Syngenetic/ Epigenetic
*Rotmistrovka, Ukraine	49°00′N; 32°00′E	2.7	Oil shale	Epigenetic
*Saint Martin, Canada	51°47′N; 98°32′W	40	Gypsum, anhydrite	Epigenetic
*Saltpan, South Africa	25°24′S; 28°50′E	1.1	Various salts	Epigenetic
Serpent Mound, USA	39°02′N; 83°24′W	8	Lead, zinc	Syngenetic
*Siljan, Sweden	61°02′N; 14°52′E	55	Lead, zinc, oil	Syngenetic/ Epigenetic
*Sierra Madera, USA	30°36′N; 102°55′W	13	Gas	Epigenetic
Slate Islands, Canada	48°40′N; 87°00′W	30	Gold	Progenetic
*Steen River, Canada	59°31′N; 117°37′W	25	Oil, gas	Epigenetic
*Sudbury, Canada	46°36′N; 81°11′W	250	Copper, nickel, PGE, Diamond	Syngenetic
*Ternovka, Ukraine	48°08′N; 33°31′E	12	Iron, uranium	Progenetic/ Syngenetic
Tookoonooka, Australia	27°00′S; 143°00′E	55	Oil	Epigenetic
*Viewfield, Canada	49°35′N; 103°04′W	2.5	Oil	Epigenetic
*Vredefort, South Africa	27°00′S; 27°30′E	300	Gold, uranium	Progenetic/ Syngenetic
Zapadnaya, Ukraine	49°44′N; 29°00′E	4	Diamond	Syngenetic
*Zhamanshin, Kazakhstan	48°24′N; 60°58′E	13.5	Bauxite, impact glass	Progenetic/ Syngenetic

*Resources exploited currently or in the past. Above listing does not include structures that are a source of fresh water, various building materials, or are used as hydroelectric reservoirs or the impact-related Cantarell oil field in Mexico.

Iron and uranium at Ternovka. Iron and uranium ores occur in the basement rocks of the crater floor and in impact breccias at the Ternovka or Terny structure, Ukraine (Table 2; Nikolsky *et al.* 1981, 1982). The structure is 375 ± 25 Ma old according to Nikolsky (1991) and was formed in a Lower Proterozoic fold belt. It is a complex crater from which erosion has removed more than 700 m, including most of the allochthonous impact lithologies, and has exposed the floor of the structure (Krochuk & Sharpton 2002). The central uplift is, in part, brecciated and injected by dykes of impact-melt rock up to 20 m wide. The annular trough contains remnants of allochthonous breccia, with patches and lenses of suevite. The present diameter of the structure is 10–11 km and its original diameter may have been 15–18 km. However, there is a smaller estimate for the original diameter of *c.* 8 km by Krochuk & Sharpton (2003), who also reported a younger, single whole rock $^{39}Ar/^{40}Ar$ date of 290 ± 10 Ma from an impact-melt rock.

The iron ores at Ternovka have been exploited through open pit and underground operations for more than fifty years. The ores are the result of hydrothermal and metasomatic action, which occurred during the Lower Proterozoic, on ferruginous quartzites (jaspilites) and some other lithologies, producing zones of albitites, aegirinites, and amphibole–magnetite and carbonate–hematite rocks, along with uranium mineralization. Post-impact hydrothermal alteration led to the remobilization of some of the uranium mineralization and the formation of veins of pitchblende. The production of uranium ceased in 1967 but iron ore was extracted, until recently, from two main open pits: Annovsky and Pezromaisk. The total reserves at the Pezromaisk open pit are estimated at 74 million tonnes, with additional reserves of lower grade deposits estimated at *c.* 675 million tonnes. Due to brecciation and displacement, blocks of iron ore are mixed with barren blocks. These blocks are up to hundreds of metres in dimension, having been rotated and displaced from their pre-impact positions. This displacement and mixing of lithologies causes difficulties in operation and evaluating the reserves but impact-induced fracturing aids in extraction and processing. Currently, mining operations are in a maintenance mode but may resume under new ownership (R. Krochuk, pers. comm. 2004).

Uranium at Carswell. The Carswell impact structure (Table 2) is located in northern Saskatchewan, Canada, approximately 120 km south of Uranium City. Details of various geological, geophysical and geochemical aspects of the Carswell structure, with heavy emphasis on the uranium ore deposits, can be found in Lainé *et al.* (1985). The Carswell structure is apparent in Shuttle Radar Topography as a two circular ridges, corresponding to the outcrop of the dolomites of the Carswell Formation (Fig. 6). The outer ridge is *c.* 39 km in diameter and is generally quoted as the diameter of the structure (e.g. Currie 1969; Innes 1964; Harper 1982). It represents a minimum original diameter. The outer ring of the structure is about 5 km wide and forms cliffs 65 m high of the Douglas and Carswell Formations. Interior to this, there is an annular trough, occupied by sandstones and conglomerates of the William River Subgroup of the Athabasca Group (Fig. 7). This trough is also approximately 5 km wide and rises to a core, *c.* 20 km in diameter, of metamorphic crystalline basement. The Carswell impact structure has been eroded to below the floor of the original crater.

The crystalline basement core consists of mixed feldspathic and mafic gneisses of the Earl River Complex, overlain by the more aluminous Peter River gneiss. Details of their mineralogy and chemistry can be found in Bell *et al.* (1985), Harper (1982), and Pagel & Svab (1985). The basement core is believed to have been uplifted by a minimum of 2 km. In a detailed structural study of the Dominique-Peter uranium deposit near the southern edge of the crystalline core, Baudemont & Fedorowich (1996) estimated that the amount of structural uplift in that area was in the order of 1.2 km. Surrounding the

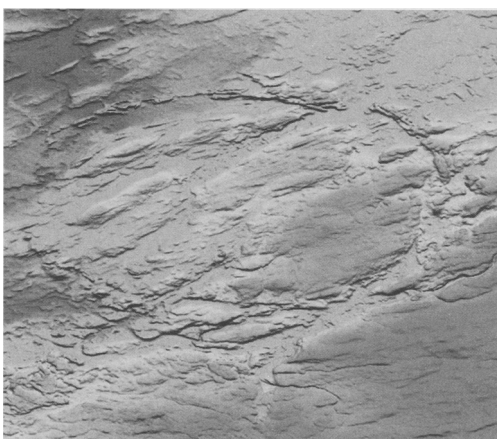

Fig. 6. Shuttle topographic radar image of digital topography over the Carswell impact structure (Table 2).

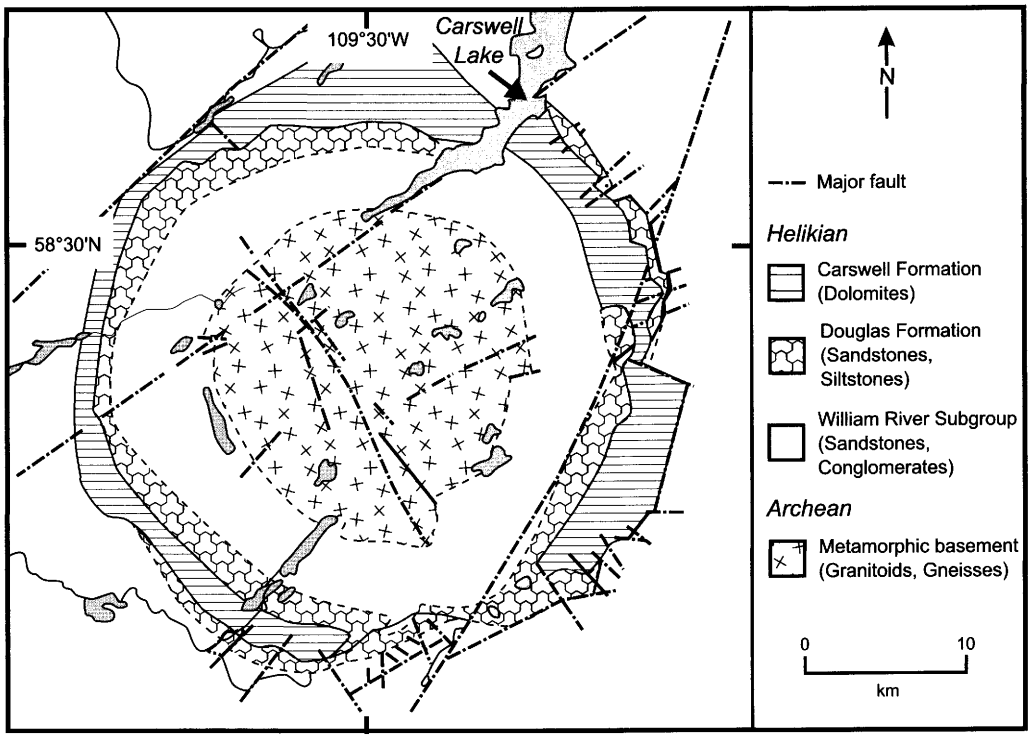

Fig. 7. Geological map of the Carswell impact structure, indicating uplifted crystalline basement core and down-faulted annulus of Carswell and Douglas Formations approximately corresponding to the circle in Fig. 14.

crystalline basement core are units of the unmetamorphosed Athabasca Group of sediments. The inner contact with the basement core is faulted and truncated in places and offset by radial faults. The outer contact of the Carswell Formation is also characterized by arcuate faulting, drag folding and local overturning of beds, as well as being offsets by radial faults (Fig. 7). There are several regional faults unrelated to the impact structure. The Carswell and Douglas Formations are the uppermost units of the Athabasca Group. Their outcrop is unique to the area and they owe their preservation to having been down-faulted at least 1 km to their present position (Harper 1982; Tona *et al.* 1985). Brecciation is common at Carswell and affects all lithologies. Currie (1969) used the term 'Cluff Breccias', after exposures near Cluff Lake, to include autochthonous monomict breccias, allochthonous polymict clastic breccias and impact melt rocks (Fig. 8). The latter two lithologies occur as dyke-like bodies and the relationships between the various breccias are locally complex (Wiest 1987).

The Athabasca Basin is the largest and richest known uranium-producing region in the world. Cumulative uranium production from the basin is approximately 1.5 billion pounds of uranium oxide, with a value of close to US$1.5 billion. Within the Carswell structure, the six known commercial uranium deposits occur in two main settings: at the unconformity between the Athabasca sandstone of the William River Subgroup and the uplifted crystalline basement core, and in mylonites and faults in the crystalline core. These deposits had grades between 0.3 and 6.8% uranium oxide and have produced close to US$70 million worth of uranium. The original uranium mineralization in the Athabasca Basin, and at Carswell, occurred during regolith development in the Precambrian, with later remobilization due to hydrothermal activity in response to thermotectonic events (Bell *et al.* 1985; Lainé 1986). The original commercial uranium deposit discovered at Carswell, the Cluff Lake D deposit, was a pre-existing or progenitic ore deposit that was brought to its present location by structural uplift in the Carswell impact event and subsequent erosion. The mineralization at

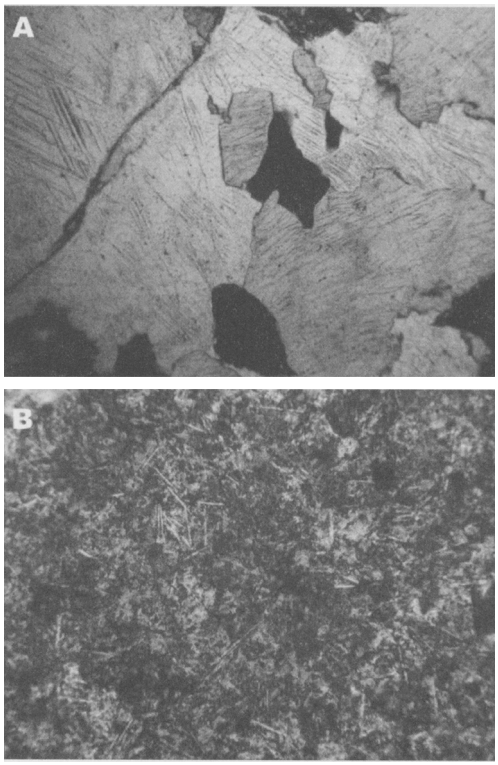

Fig. 8. Photomicrographs of lithologies at Carswell. (**A**) Planar deformation features in quartz in crystalline basement core. (**B**) Impact melt rock with aphanitic matrix and acicular feldspar. Crossed polars, fields of view 1 mm.

Cluff Lake D is also associated with shear zones and faulting (Tona *et al.* 1985). At the time of mining, it was the richest uranium ore body in the world (Lainé 1986).

In their detailed structural study of Dominique-Peter, the largest basement-hosted deposit, Baudemont & Fedorowich (1996) recognized four episodes of deformation. Two of these were prior to mineralization, the third episode related to mineralization and the final episode related to the Carswell impact event. They note that Carswell-related deformation reactivated earlier faults associated with the main mineralization. In addition, the paragenesis of the basement-hosted ore bodies contrasts with the other unconformity-type deposits of the Athabasca Basin and the Cluff D deposit at Carswell, in that they are vein-type deposits, related to fault zones reactivated by the Carswell impact. 'Cluff Breccia' also commonly occurs in the same fault structures as the uranium mineralization. Baudemont & Fedorowich (1996) found the association 'striking, albeit complexing'. Mineralized material occurs within the Cluff Breccias, which are, themselves, mineralized with veins of coffinite (Lainé 1986).

It is not clear to what extent the Carswell impact event was involved in remobilizing the ores, beyond physical movement associated with fault reactivation during structural uplift. The basement-hosted ores are all associated with extensive alteration, indicative of hydrothermal fluid movement (Lainé 1986). At present, the last of the known commercial uranium deposits within the Carswell structure is in the mine-decommissioning phase. However, there are additional known exploration targets and reactivated faults, with pseudotachylite and/or 'Cluff Breccias' and uranium mineralization, are considered to be good future exploration drill targets (Baudemont & Fedorowich 1996).

Gold and uranium of Vredefort. The Vredefort structure, South Africa (Table 2), consists of an uplifted central core of predominantly Archaean granites (44 km in diameter) surrounded by a collar of steeply dipping to overturned Proterozoic sedimentary and volcanic rocks of the Witwatersrand and Ventersdrop Supergroup (18 km wide) and an outer broad synclinorium of gently dipping Proterozoic sedimentary and volcanic rocks of the Transvaal Supergroup (28 km wide). Younger sandstones and shales of the Karoo supergroup cover the southeastern portion of the structure. The general circular form with an uplifted central core, the occurrence of stishovite and coesite, as well as planar deformation features in quartz and shatter cones have all been presented as evidence that the Vredefort structure is the eroded remnant of a very large, complex impact structure (e.g. Dietz 1961; Hargraves 1961; Carter 1965; Manton 1965, Martini 1978, 1991; Gibson & Reimold 2000).

The Witwatersrand Basin (Fig. 9) is the world's largest goldfield, having supplied some 40% of the gold ever mined in the world. Since gold was discovered there in 1886, it has produced 47 000 tonnes of gold. The annual Witwatersrand gold production for 2002 was approximately 350 tonnes, or approximately 13.5% of the global gold supply, and current reserve estimates are around 20 000 tonnes of gold. The Vredefort impact event, occurred at 2023 ± 4 Ma. Based on the spatial distribution of impact-related deformation and structural features, Therriault *et al.* (1997) derived a self-consistent, empirical estimate of the original size of the Vredefort impact structure at

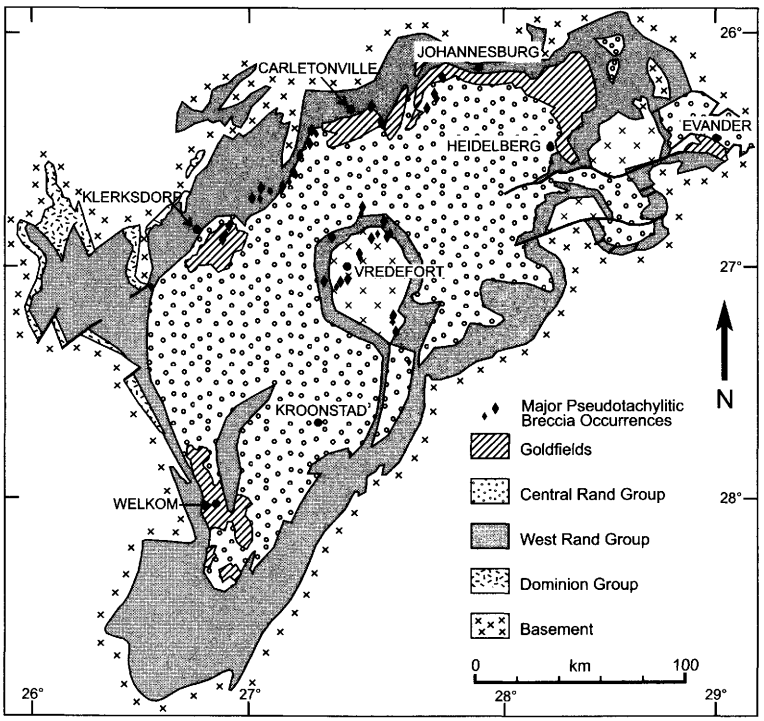

Fig. 9. Geological map of the Witwatersrand Basin, with partially obscuring Karoo Supergroup removed, indicating the central location of Vredefort.

between 225–300 km in diameter. A similar size estimate was derived by Henkel & Reimold (1998), based on potential field and reflection seismic data. These estimates effectively equate the spatial extent of the Vredefort impact structure to the entire Witwatersrand Basin (Fig. 10).

Independent of impact studies at Vredefort, structural analyses have identified a series of concentric anticlinal and synclinal structures related to Vredefort (e.g. McCarthy *et al.* 1986, 1990). The preservation of progenitic ores from erosion in these Vredefort-related structures (McCarthy *et al.* 1990) provided the emphasis for Grieve & Masaitis (1994). The origin of the gold in the Basin is still debated, with pure detrital and hydrothermal models and combinations of the two (e.g. Barnicoat *et al.* 1999; Minter 1999; Phillips & Law 2000). Gold with clear detrital morphological features (Minter *et al.* 1993), occurs with secondary, remobilized gold. This suggests that detrital gold was introduced into the Basin but that some gold was subsequently remobilized by hydrothermal activity. Grieve & Masaitis (1994) speculated that some remobilization of uranium may have occurred due to the Vredefort event but were equivocal as to the role of thermal activity resulting from the spatially and temporally (2.05–2.06 Ga) close igneous event associated with the Bushveld Complex. Recent work has clarified the situation, with the Vredefort impact event forming both an important temporal marker and a critical element in the process of gold remobilization.

Two thermal or metamorphic events affected the rocks of the Basin. A regional amphibolite facies metamorphism predates the Vredefort impact event. However, a later, low pressure (0.2–0.3 GPa), post-impact event produced peak temperatures of 350 ± 50 °C in the Witwatersrand Supergroup to >700 °C in the centre of the crystalline core at Vredefort (Gibson *et al.* 1998). This post-impact metamorphism, which increased in intensity radially inwards, explains the previously documented progressive annealing of PDFs in the core rocks (Grieve *et al.* 1990) and is directly attributed to the combination of post-shock heating and the structural uplift of originally relatively deep-seated parautochthonous rocks during the Vredefort impact event (Gibson *et al.* 1998).

This post-impact metamorphism can be regarded as an integral part of the Vredefort impact event (Gibson & Reimold 1999). The

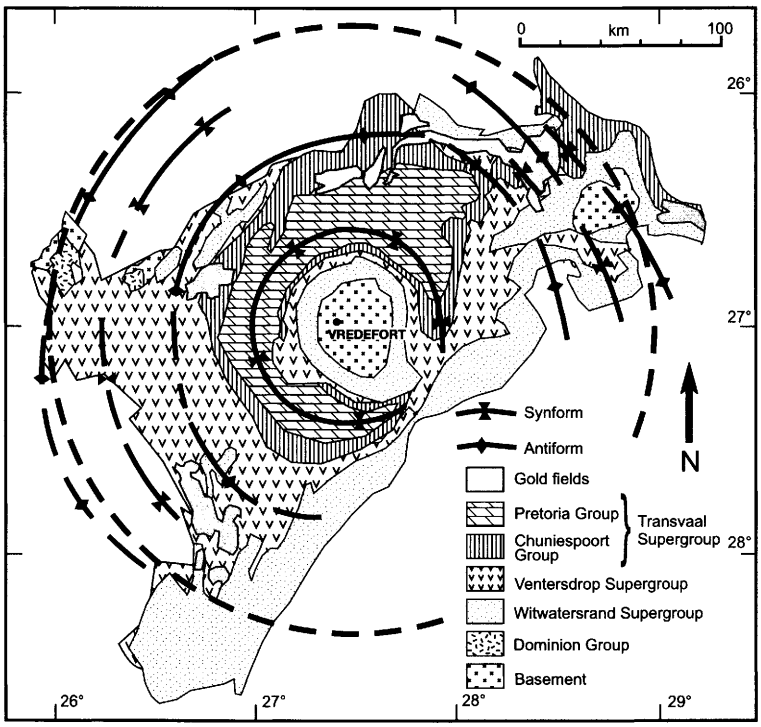

Fig. 10. Distribution of large concentric structures and gold fields, with respect to a 300 km diameter (dashed line) impact structure centred on Vredefort (Table 2).

heat engine that drove post-impact hydrothermal activity was a result of the impact. Brecciation and the formation of pseudotachylite and other breccia dykes in the impact event also provided channels for fluid migration. Reimold *et al.* (1999) coined the term 'autometasomatism' to describe the associated chlorite ± sericite alteration associated with the hydrothermal activity, in response to the thermal anomaly in the parautochthonous rocks of the basin and resulting from the Vredefort impact. This activity remobilized gold (and uranium) within impact-related structures and fractures, on all scales, that provided channels for fluid migration (Reimold *et al.* 1999). These fluids appear to have been originally meteoric and local in origin; gold was associated with chlorite and quartz veins, for example in the Ventersdrop Contact Reef (Frimmel *et al.* 1999). It is now evident the Vredefort impact event played a larger role in the genesis of the Witwatersrand Basin gold fields than simply preserving them from erosion by structural modification (McCarthy *et al.* 1990; Grieve & Masaitis 1994).

Syngenetic deposits

Syngenetic economic natural resources at impact structures include impact diamonds, Cu–Ni sulphides and platinum-group and other metals (Tables 1 & 2).

Impact diamonds. The first indication of impact diamonds was the discovery in the 1960s of diamond with lonsdaleite, a high-pressure (hexagonal) polymorph of carbon, in placer deposits, e.g. in the Ukraine, although their source was unknown (Cymbal & Polkanov 1975). In the 1970s, diamond with lonsdaleite was discovered in the impact lithologies at the Popigai impact structure. Since then, impact diamonds have been discovered at a number of structures, e.g. Kara, Lappajärvi, Puchezh-Katunki, Ries, Sudbury, Ternovka, Zapadnaya, and others (Gurov *et al.* 1996; Langenhorst *et al.* 1998; Masaitis 1993, 1998; Siebenschock *et al.* 1998).

Impact diamonds originate as a result of phase transitions from graphite, or crystallization from coal, and occur when their precursor carbonaceous lithologies were subjected to shock pressures > 35 GPa (Masaitis 1998). The

diamonds from graphite in crystalline targets usually occur as paramorphs, with inherited crystallographic features (Masaitis *et al.* 1990; Val'ter *et al.* 1992) and as microcrystalline aggregates. At Popigai, these aggregates can reach 10 mm in size but most are 0.2–5 mm in size (Masaitis 1998). They consist of cubic diamond and lonsdaleite, with individual microcrystals of 10^{-4} cm. The diamonds, generated from coal or other carbon in sediments, are generally porous and coloured.

Diamonds are most common as inclusions in impact-melt rocks and glass clasts in suevite breccias. For example at Zapadnaya, Ukraine, they occur in impact-melt dykes in the central uplift and in suevite breccias in the peripheral trough (Gurov *et al.* 1996). Zapadnaya, *c.* 3.8 km in diameter, 115 ± 10 Ma old, was formed in Proterozoic granite containing graphite (Gurov *et al.* 1985). At Popigai (Table 2), the allochthonous breccia filling the peripheral trough is capped by diamond-bearing suevites and coherent bodies of impact-melt rocks (Fig. 11). The largest of these melt-rock bodies can be traced for 10–15 km along strike and is 500 m thick (Fig. 12; Masaitis *et al.* 1980). In the case of Popigai, the original source of the carbon is Archaean gneisses with graphite. The diamonds at Kara, Russia, also occur in impact-melt rocks. Kara, 65 km in diameter, 67 ± 6 Ma old, is located in a Palaeozoic fold belt, which contains Permian terrigenous sediments containing coal (Ezerskii 1982). Impact diamonds can also be found in strongly shocked lithic clasts in suevite breccias, e.g. at Popigai and Ries (Masaitis 1998; Siebenschock *et al.* 1998). In impact-melt rocks at structures with carbon-bearing lithologies, diamonds occur in relatively minor amounts, with provisional average estimates in the order of 10 ppb, although the cumulative volumes can be enormous. Although diamonds associated with known impact structures are not currently

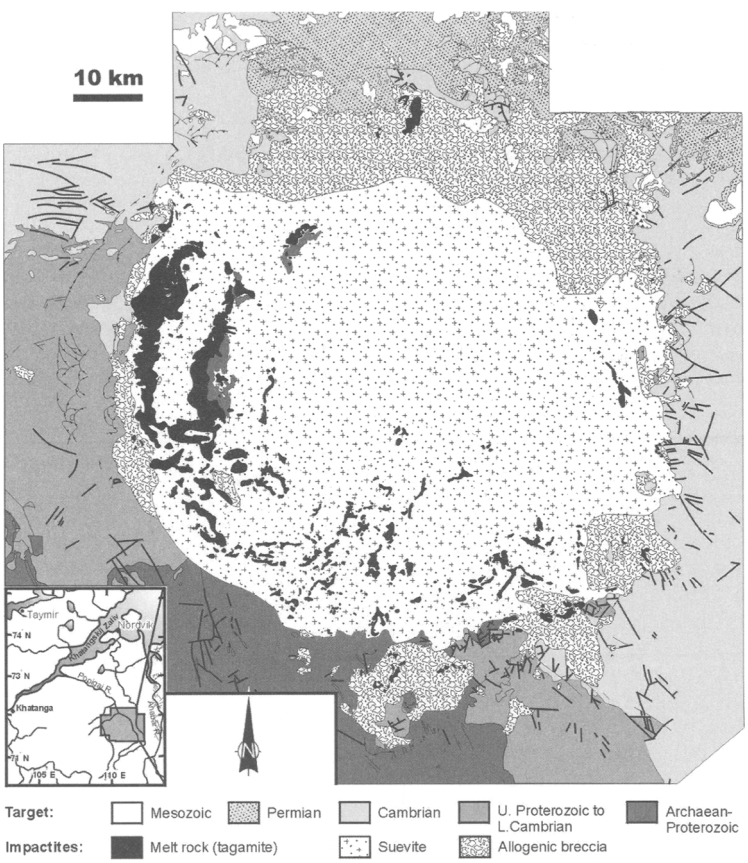

Fig. 11. Geological map of the Popigai impact structure (Table 2) indicating the distribution of impact melt rocks and suevite.

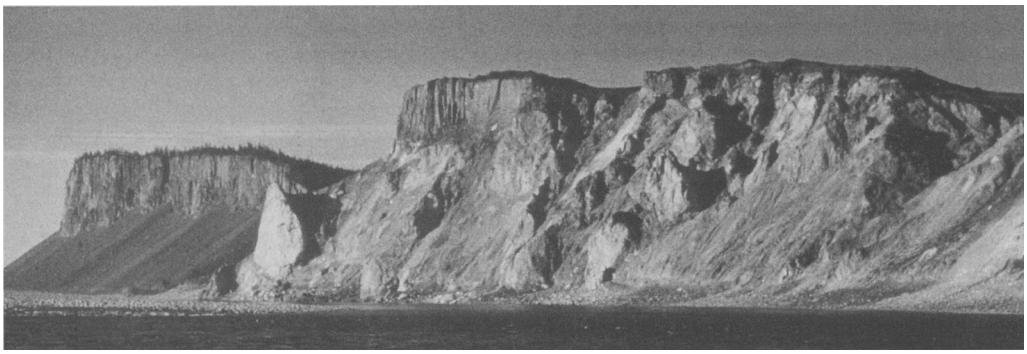

Fig. 12. Field photograph of outcrop of the sheet of diamond-bearing impact melt rocks, overlying allochthonous breccia, at the Popigai impact structure, Cliffs are approximately 150 m high.

exploited commercially, those produced by shock transformation of graphite tend to be harder and more resistant to breaking than the normal cubic diamonds from kimberlites.

At the Ries, Hough *et al.* (1995) have reported the only known occurrence of impact cubic diamond from impact lithologies, again suevite. They also reported the occurrence of SiC grains. The cubic diamonds are skeletal in appearance and they attributed their origin, and that of the SiC, to chemical vapour deposition in the ejecta plume over the impact site. Based on carbon isotope studies, they considered the source of the carbon and other elements to be from sedimentary rocks, including carbonates, which overlay the crystalline basement at the time of Ries impact and calculated that the Ries suevite might contain 7.2×10^4 tonnes of diamonds and SiC, in the proportion of 3:1. Other workers (e.g. Siebenschock *et al.* 1998) failed to find either cubic diamond or SiC at the Ries. Silicon carbide, however, has been reported from the Onaping Formation at the Sudbury impact structure (Masaitis *et al.* 1999). In this location, it is associated with impact diamonds that are a mixture of cubic diamond and hexagonal lonsdaleite, resulting not from chemical vapour deposition but from solid-state transformation by shock of precursor graphite.

Cu–Ni sulphides and platinum group metals at Sudbury. The Sudbury structure, Canada (Table 2), is the site of world-class Ni–Cu sulphide and platinum group metal ores. The pre-mining resources at Sudbury are estimated at 1.65×10^9 tonnes of 1.2% Ni and 1.1% Cu (Naldrett & Lightfoot 1993) and are associated with the Sudbury Igneous Complex (SIC). Sulphides were first noted at Sudbury in 1856. It was not until they were 'rediscovered' during the building of the trans-Canada railway in 1883 that they received attention, with the first production occurring in 1886 (Naldrett 2003). By 2000, the Sudbury mining camp had produced 9.7 million tonnes of Ni, 9.6 million tonnes of Cu, 70 thousand tonnes of Co, 116 tonnes of Au, 319 tonnes of Pt, 335 tonnes of Pd, 37.6 tonnes of Rh, 23.3 tonnes of Ru, 11.5 tonnes of Ir, 3.7 thousand tonnes of Ag, 3 thousand tonnes of Se and 256 tonnes of Te (Lesher & Thurston 2002).

The most prominent feature of the Sudbury structure is the *c.* 30 × 60 km elliptical basin formed by the outcrop of the SIC, the interior of which is known as the Sudbury Basin (Figs 13 & 14). Neither the SIC nor the Sudbury Basin are synonymous with the Sudbury impact structure. The Sudbury impact structure includes the Sudbury Basin, the SIC and the surrounding brecciated basement rocks and covers a present area of > 15 000 km^2 (Giblin 1984*a*,*b*). From the spatial distribution of shock metamorphic features (e.g. shatter cones; Fig. 15) and other impact related attributes and by analogy with equivalent characteristics at other large impact structures, Grieve *et al.* (1991) estimated that the original crater rim diameter was 150–200 km. Central to these estimates is the assumption that the SIC was originally circular and, at its present level of erosion, was 60 km in diameter.

The elliptical shape of the Sudbury Basin is due to deformation caused by the Penokean Orogeny (Rousell 1984). The extent of this deformation was only recently appreciated. The results of a reflection seismic traverse across the Sudbury Basin, in the course of a LITHOPROBE transect, indicated NW thrusting (Milkereit *et al.* 1992; Wu *et al.* 1995). Additional works (Cowan & Schwerdtner 1994; Hirt *et al.*

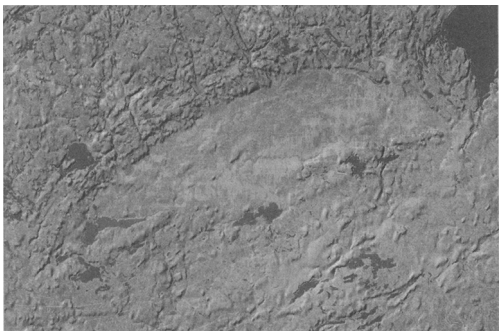

Fig. 13. Digital elevation image of the centre of the Sudbury impact structure (Table 2). The Sudbury Igneous Complex appears as a NE–SW orientated elliptical body *c.* 30 × 60 km in diameter, enclosing the smoother terrain of the Sudbury Basin. Traces of NNW trending faults can be clearly seen cutting the North Range of the Sudbury Igneous Complex. Arcuate structures associated with the superimposed younger Wanapitei impact structure are visible in the NW corner of the image. Source: V. Singhroy, Canada Centre for Remote Sensing.

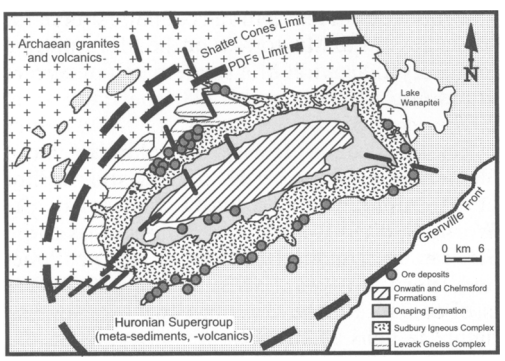

Fig. 14. Simplified regional geological map of the area of the Sudbury Igneous Complex, indicating major lithological Precambrian provinces (Archaean, Huronian, Grenville), Sudbury Igneous Complex and post-impact Whitewater Series of the Sudbury Basin. Dashed lines are prominent faults of varying age. Also indicated are the limits of the occurrence of shock metamorphic features (shatter cones, PDFs) and major ore deposits.

1993) indicated that there was a significant component of ductile deformation prior to the thrusting and brittle deformation. The original diameter of the SIC, at its present level of erosion, may have been 75–80 km and would have extended the original diameter of the final rim of the structure to the 250 km range (Deutsch & Grieve 1994; Stöffler *et al.* 1994). Even larger original diameters have been

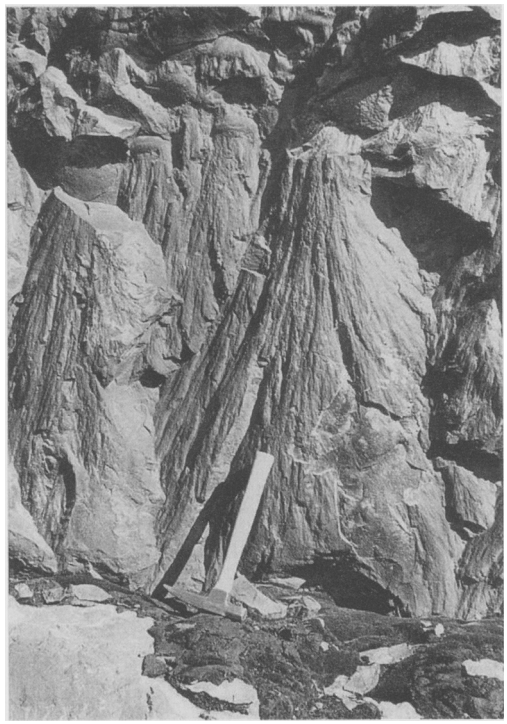

Fig. 15. Shatter cones in Huronian quartzite at the Sudbury impact structure.

suggested (e.g. Naldrett 2003; Tuchsherer & Spray 2002). There is some thermal disturbance of $^{40}Ar/^{39}Ar$ ages of Sudbury-related pseudotachylite north of the SIC, which suggest that there may be previously unrecognized post-impact Penokean metamorphism and possibly tectonic shortening in the north, in addition to the observed shortening in the south (Thompson *et al.* 1998). With the tectonic deformation and the considerable erosion, estimated to be *c.* 10 km (Schwarz & Buchan 1982), that has taken place at the Sudbury impact structure, it is difficult to constrain its original form. From its estimated original dimensions, it was most likely a peak-ring or a multi-ring basin (Stöffler *et al.* 1994; Spray & Thompson 1995).

Details of the geology of the Sudbury structure and the general area can be found in Dressler (1984*a*). In the simplest terms, the target rocks consisted of Archaean granite–greenstone terrain of the Superior Province of the Canadian Shield overlain, at the time of impact, by 5–10 km of Proterozoic Huronian metasediments, mostly arenaceous quartzites and wackes, and metavolcanics. The present outcrop pattern is illustrated in Figure 14, which

also indicates the outcrop of Grenvillian gneisses to the SE, that were not present at the time of impact. North of the SIC, the presently exposed target rocks are Archaean granite–greenstones with a partial ring of down-dropped Huronian metasediments (Fig. 14). Closer to and immediately adjacent to the, so-called, North Range of the SIC, the relatively low grade granite–greenstone is replaced by the amphibolite facies rocks and, closest to the SIC, granulite facies Levack Gneiss Complex. These gneisses are complex, in detail, and have been thermally metamorphosed for a distance of > 1 km by the SIC (Dressler 1984*b*). The Levack gneisses formed at depths of 21–28 km (James *et al.* 1992). It is not certain that they were uplifted to their present position by the Sudbury impact event but uplift of this magnitude (*c.* 26 km) is presumed from an impact structure 250 km in diameter, based on empirical relations at other large impact structures (Grieve & Therriault 2004). Preliminary $^{40}Ar/^{39}Ar$ ages on hornblende separates from the Levack gneisses are consistent with uplift as a result of the Sudbury impact event (N. Wodicka, personnal communication, 2003). To the south and west, the footwall of the SIC is largely Huronian metasediments and metavolcanics (Fig. 14), but also includes Proterozoic granitic plutons.

The SIC has been subdivided into a number of phases or units. At the base, there is the Contact Sublayer (Fig. 16). This is the host to much of the sulphide mineralization at Sudbury. The sublayer has an igneous-textured matrix (Pattison 1979; Naldrett *et al.* 1984). Inclusions are of locally derived target rocks and mafic to ultramafic rocks. Recent U–Pb dating of these mafic inclusions indicates an age equivalent to that of the SIC, suggesting that it may represent materials that crystallized at an early stage from the SIC (Corfu & Lightfoot 1996). Generally included with the sublayer are the so-called Offset Dykes of the SIC (Naldrett *et al.* 1984). These dykes are most often radial to the SIC but some are concentric and they are hosts to Ni–Cu sulphide deposits. Some are extensive, e.g. the Foy Offset can be traced for *c.* 30 km from the North Range of the SIC and ranges from approximately 400 m in width near the SIC to 50 m at its most distal part (Grant & Bite 1984; Tuchscherer & Spray 2002).

Stratigraphically above the Sublayer lies the Main Mass of the SIC (Fig. 16), which is relatively, but not completely, clast free. For example, there are rare quartz clasts with partially annealed PDFs (Therriault *et al.* 2002). The contact relations between the sublayer and the Main Mass are apparently contradictory in places, with inclusions of Main Mass in the sublayer and vice versa (Naldrett 1984). Traditionally, the Main Mass has been divided into a number of facies: mafic norite, quartz-rich norite, felsic norite, quartz gabbro and granophyre, depending on the mineralogy. These facies are actually misnomers on the basis of the modal quartz, alkali feldspar and plagioclase proportions, as plotted on a Streckeisen diagram. Only the sublayer is gabbroic, the others fall in the quartz gabbro, quartz monzogabbro, granodiorite, and granite fields (Therriault *et al.* 2002). The nomenclature confusion arises from the fact that, like most impact melts of granitic/granodioritic composition, the mafic component of the melt crystallized as ortho-, and clino-pyroxene; although, there are also primary hydrous amphibole and biotite. Therriault *et al.* (2002), who made their observations on continuous cores rather than discontinuous outcrop, also demonstrated, on the basis of both mineralogy and geochemistry, that the contacts between the various facies of the SIC are gradational. The details of the mineralogy and geochemistry support a cogenetic source for the facies of the Main Mass of the SIC and fractional crystallization of a single batch of silicate liquid (e.g. Warner *et al.* 1998; Therriault *et al.* 2002).

The most comprehensive survey of the major element chemistry of the SIC is still Collins (1934), although more recent analyses of the Worthington Offset Dyke and Main Mass of the SIC can be found in Lightfoot & Farrow (2002) and Therriault *et al.* (2002), respectively. There is, of course, a massive proprietary geochemical database held by the mining companies in the area. The most unusual character of the average composition of the SIC is its high SiO_2 and K_2O, depletion in CaO and a low Na_2O/K_2O ratio compared to magmatic rocks of similar Mg number (Naldrett & Hewins 1984; Naldrett 1984). It also has an REE pattern, which is enriched in light rare earths (Kuo & Crockett 1979; Faggart *et al.* 1985), and is essentially that of the upper continental crust (Fig. 17; Faggart *et al.* 1985; Grieve *et al.* 1991). To account for these characteristics, earlier proponents of a magmatic origin for the SIC had to call upon massive crustal contamination of a mantle-derived magma (Kuo & Crockett 1979; Naldrett & Hewins 1984; Naldrett 1984). Strong arguments against such a proposal come from isotopic data and from thermal constraints. The $(^{87}Sr/^{86}Sr)^{T=1.85\ Ga}$ ratios for various lithologies of the SIC cluster at 0.707 but can range as high as 0.710 for granophyre samples (Gibbins &

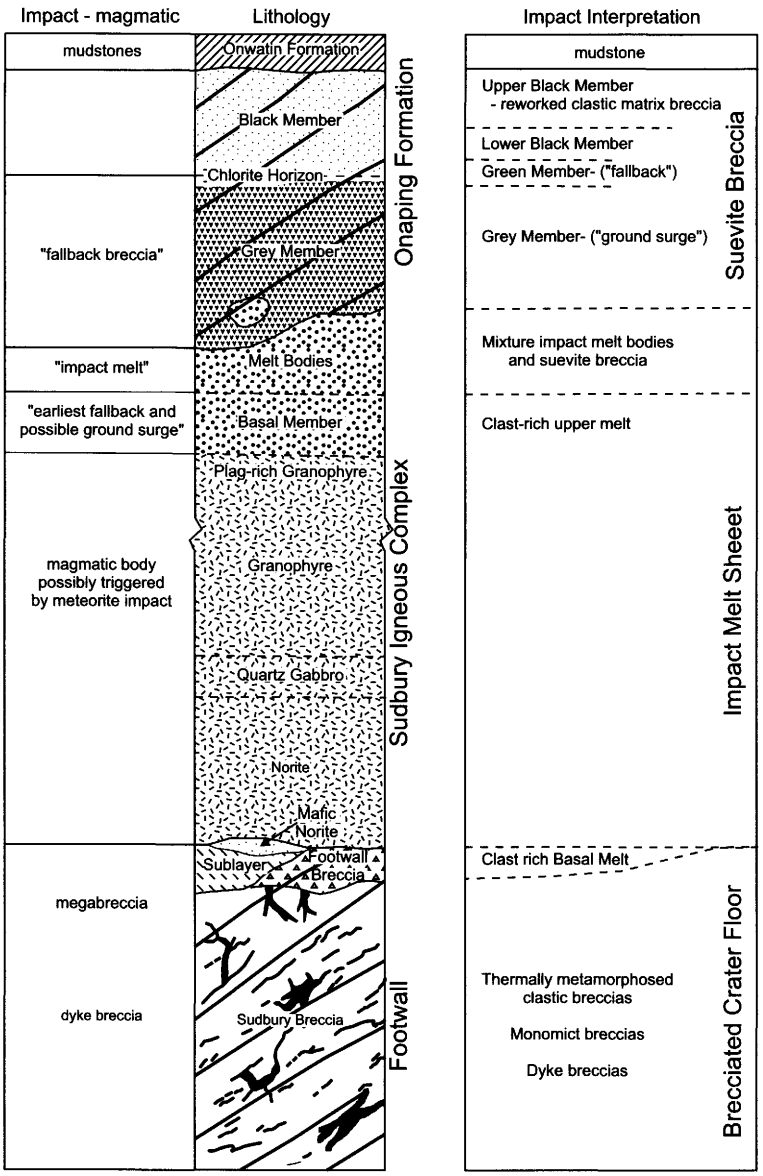

Fig. 16. Schematic stratigraphic section (not to scale) of lithologies at the Sudbury impact structure, with traditional nomenclature. Left-hand column is hybrid impact-magmatic interpretation of their genesis. Right-hand column is solely impact interpretation.

McNutt 1975; Hurst & Farhat 1977) or up to 0.7175 for the sublayer in the South Range (Faggart *et al.* 1985; Ostermann *et al.* 1996; Morgan *et al.* 2002*b*). The SIC is isotopically dated at 1.85 Ga (Krogh *et al.* 1984). These values are not compatible with a mantle-derived intrusion with a 1.85 Ga age. A similar argument holds for Nd isotopic systematics. Faggart *et al.* (1985) determined $Nd^{T=1.85\ Ga}$ values of –7 to –8.8 for different units of the SIC that are typical for average upper continental crust at that time.

The conclusion that the SIC and its ores are not mantle-derived but crustal in composition is borne out by other isotopic studies (e.g. Fig. 18; Dickin *et al.* 1992, 1996, 1999; Walker *et al.* 1991). Cohen *et al.* (2000) analysed the Re–Os isotopes in the ultramafic inclusions in the sublayer of the

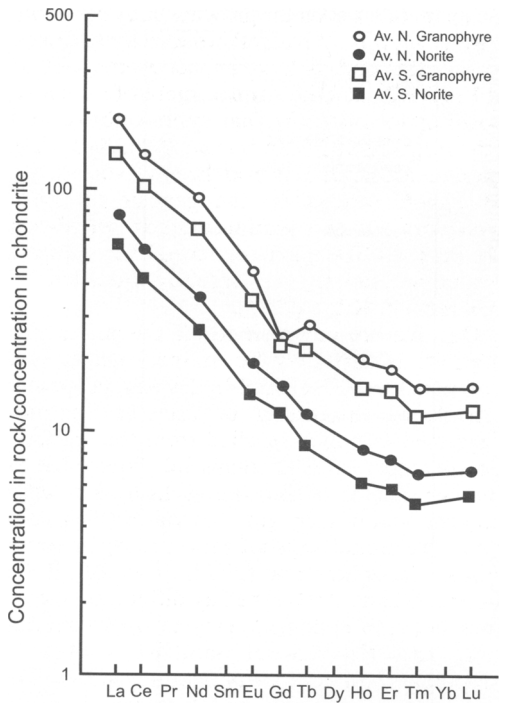

Fig. 17. Normalized REE abundances in phases of the Sudbury Igneous Complex lithologies of the North and South Ranges, indicating a crustal REE pattern for the Sudbury Igneous Complex. Source: Therriault *et al.* (2002).

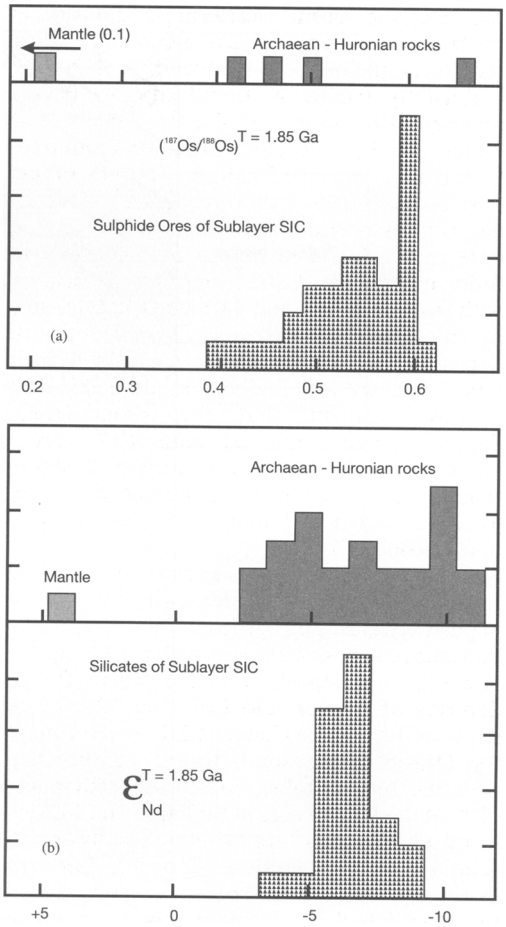

Fig. 18. Plot of (**a**) osmium and (**b**) neodymium isotopic data of ores and silicates in sublayer of the Sudbury Igneous Complex, compared to local crustal sources in the area of the Sudbury impact structure and the mantle at 1.85 Ga. Source: Faggart *et al.* (1985), Dickin *et al.* (1996, 1999).

SIC and concluded that they were also consistent with melting of pre-existing lithologies at 1.85 Ga. They also produced an imprecise crystallization age of 1.97 $\pm$ 0.12 Ga, which is within the error of 1.85 Ga crystallization age of the SIC, from a number of the inclusions. Recent, high precision Os isotope studies of sulphides from several mines have confirmed their crustal origin from a binary mixture of Superior Province and Huronian metasedimentary rocks (Morgan *et al.* 2002*b*).

There is a considerable geophysical database for the Sudbury impact structure. Most of the geophysical data are concentrated around the SIC and within the Sudbury Basin, because of the ore deposits, and a great deal of the data are proprietary. Most recently, the area around the SIC has been the subject of multidisciplinary geophysical studies, as part of a LITHOPROBE transect in the area. A north–south profile was completed in 1991 and additional data were acquired over parts of the South Range of the SIC in 1993. The north–south profile, which consisted of more than 100 km of conventional and 40 km of high frequency Vibroseis seismic reflection data, has provided considerable insight into the structure of the SIC and the Sudbury Basin at depth (Milkereit *et al.* 1992; Wu *et al.* 1995; Boerner *et al.* 1999). These have been complemented with a variety of other geophysical data. The interpretation of these data can be found in *Geophysical Research Letters*, **21**, 1994. The combination of known ore deposits and reflection seismic data has also led Sudbury to be chosen as the first test site for the use of 3D reflection seismic survey methods for detecting massive sulphide deposits in crystalline rocks. The experiment concluded that such massive sulphide bodies produce a

characteristic seismic scattering response and the technique has potential as a new exploration tool in crystalline rocks (Milkereit *et al.* 2002).

Recently, Farrow & Lightfoot (2002) have reviewed the nature of the ore deposits at Sudbury and placed their formation in an integrated time-sequence model. As with others (e.g. Naldrett 1984), they recognize: 'Contact' deposits associated with embayments at the base of the SIC and hosted by sublayer and footwall breccia; 'Offset' deposits associated with discontinuities and variations in thickness in the offset dykes; and Cu-rich footwall deposits. They also recognize a fourth deposit type associated with Sudbury Breccia. This is an acknowledgement that the Frood-Stobie deposit, which contained some 15% of the known mineralization and produced 600 million tonnes of ore, is not hosted in a traditional offset dyke but rather in Sudbury Breccia (Scott & Spray 2000).

The contact deposits consist of massive sulphides and are volumetrically the largest deposit-type, hosting approximately 50% of the known ore deposits. They include the Creighton and Whistler deposits and the North Range deposits of Levack and Coleman. The offset deposits include the Copper Cliff and Worthington Offsets in the South Range, which, along with the Frood-Stobie, contain approximately 40% of the known ores at Sudbury. The Cu-rich footwall deposits are volumetrically small relative to the contact deposits but are extremely valuable ore bodies, as they are relatively enriched in platinum group metals, in addition to copper. This type of deposit is hosted in the brecciated footwall of the SIC and is best known in the North Range, e.g. McCreedy East and West, Coleman, Strathcona and Fraser, where they occur as complex vein networks.

There is increasing realization that hydrothermal remobilization played a role in the genesis of the footwall deposits (e.g. Carter *et al.* 2001; Farrow & Watkinson 1997; Marshall *et al.* 1999; Molnar *et al.* 1997, 1999, 2001). Although Farrow & Lightfoot (2002) note the importance of this hydrothermal activity, they are equivocal as to the timing and suggest it may be related to regional metamorphic events. The fluids responsible for remobilization were saline, Cl-rich and oxidizing, and were initially at temperatures in excess of 300–400 °C. As Magyarosi *et al.* (2002) noted, the Sudbury impact event occurred before the peak of Penokean metamorphism in the area. Thus the regional metamorphism could not have been responsible for the hydrothermal activity that resulted in the remobilization of metals, particularly the copper and platinum group metals. Given the growing body of knowledge in support of hydrothermal activity driven by the end result of large impact events, such as at Vredefort, and the emplacement of a massive post-impact hydrothermal system above and driven by the SIC (Ames *et al.* 1998, 2005), it is presumed that this was also the case beneath the SIC, with respect to the genesis of these secondary Cu and platinum group metal-rich ore deposits. The impact-induced hydrothermal system at Sudbury was recently modelled by Abramov & Kring (2004).

One feature common to all the major ore deposits is that they lie at the base or just beneath the SIC (Fig. 14). Earlier magmatic models of the origin of ores at Sudbury suggested that they resulted from the segregation of sulphides as an immiscible liquid, due to the assimilation of siliceous rocks by a basaltic magma, followed by gravitational settling and, later, fractional crystallization and, in some cases, remobilization (Naldrett *et al.* 1984; Morrison *et al.* 1994). The key difference, therefore, between endogenic magma with assimilation and the impact models is that a 'disequilibrium' composition, with respect to the expected equilibrium crystallization of endogenic silicate melts, was an original property of the SIC. That the metals in the ores, as well as the associated silicates, have an original crustal source is indicated by the Re–Os isotopic composition of the ores and the Nd–Sm composition of the silicates accompanying the ores (Fig. 18; Dickin *et al.* 1992). Although some details are still to be determined, recent work at Sudbury can mostly be fitted into the framework of the formation of a 200–250 km impact basin 1.85 Ga ago, with accompanying massive crustal melting producing a superheated melt of an unusual composition, which gave rise to immiscible sulphides that gravitionally settled, resulting ultimately in the present ore deposits. Complicating factors, but essential components of the evolutionary history, are the creation of a 'local' hydrothermal system resulting from the impact and the deformation by the Penokean orogeny that took place shortly after the impact.

Epigenetic deposits

Epigenetic deposits are due to the fact that impact structures can result in isolated topographic basins or locally influence underground fluid flow. Such deposits may originate almost immediately or over an extended period after the impact event and may include reservoirs of liquid and gaseous hydrocarbons, oil shales,

various organic and chemical sediments, as well as flows of fresh and mineralized waters (Tables 1 & 2).

Hydrocarbons. Hydrocarbons occur at a number of impact structures. In North America, approximately 50% of the known impact structures in hydrocarbon-bearing sedimentary basins have commercial oil and/or gas fields.

The Ames structure (Table 2) is located in Oklahoma, USA, and is a complex impact structure about 14 km in diameter, with a central uplift, an annular trough, and slightly uplifted rim. It is buried by up to 3 km of Ordovician to Recent sediments (Carpenter & Carlson 1992). The structure was actually discovered in the course of oil exploration (Roberts & Sandridge 1992) and is the principal subject of a compilation of research papers (Johnson & Campbell 1997). The rim of the structure is defined by the structurally elevated Lower Ordovician Arbuckle dolomite; more than 600 m of Cambro-Ordovician strata and some underlying basement rocks are missing in the centre of the structure due to excavation. The entire structure is covered by Middle Ordovician Oil Creek shale, which forms both the seal and source for hydrocarbons and may have produced as much as 145 million barrels of oil (Curtiss & Wavrek 1997).

The first oil and gas discoveries were made in 1990 from an approximately 500 m thick section of Lower Ordovician Arbuckle dolomite in the rim (Fig. 19). Due to impact-induced fracturing and karsting, the Arbuckle dolomite in the rim of Ames has considerable economic potential. For example the 27-4 Cecil well, drilled in 1991, had drill stem flow rates of 3440 million cubic feet of gas and 300 barrels of oil per day (Roberts & Sandridge 1992). Wells drilled in the centre failed to encounter the Arbuckle dolomite and bottomed in granite breccia of the central uplift or, closer to the rim, and the granite–dolomite breccia. These central wells (Fig. 19) produce over half the daily production from Ames and include the famous Gregory 1-20, which is the most productive oil well from a single pay zone in Oklahoma at more than 100 000 barrels of oil per year (Carpenter & Carlson 1997). Gregory 1-20 encountered a *c.* 80 m section of granite breccia below the Oil Creek shale, with very effective porosity. A drill-stem test of the zone flowed at approximately 1300 barrels of oil per day, with a conservative estimate of primary recovery in excess of 5 million barrels from this single well (Donofrio 1998). Approximately 100 wells have been drilled at Ames, with a success rate of 50%. These wells produce more than 2500 barrels of oil and more than 3 million cubic feet of gas per day. Conservative estimates of primary reserves at Ames suggest they will exceed 25–50 million barrels of oil and 15–20 billion cubic feet of gas (Donofrio 1998; Kuykendall *et al.* 1997). Hydrocarbon production is from the Arbuckle dolomite, the brecciated granite and granite–dolomite breccia and is largely due to impact-induced fracturing and brecciation, which has resulted in significant porosity and permeability.

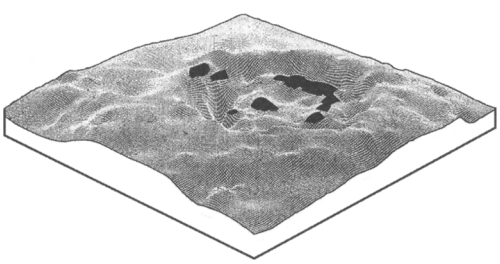

Fig. 19. Three-dimensional mesh diagram of residual structure on the post-impact upper Ordovician Sylvan shale at Ames impact structure (Table 2). View is to the NW at 25° elevation, with 20 times vertical exaggeration. Solid areas indicate where hydrocarbons are produced. Source: Carpenter & Carlson (1997).

In the case of Ames, the impact not only produced the required structural traps but also the palaeoenvironment for the deposition of post-impact shales that provided oil and gas, upon subsequent burial and maturation (Curtiss & Wavrek 1997). There are similarities between the Ames crater shale and locally developed Ordovician shale in the Newporte structure (North Dakota), an oil-producing 3.2 km diameter impact crater (*c.* 120 000 barrels per year) in Precambrian basement rocks of the Williston Basin (Donofrio 1998). The Ames and Newporte discoveries have important implications for oil and gas exploration in crystalline rock underlying hydrocarbon-bearing basins. Donofrio (1981, 1997) first proposed the existence of such hydrocarbon-bearing impact craters and that major oil and gas deposits may occur in brecciated basement rocks.

At the Red Wing Creek structure in North Dakota, USA, hydrocarbons are also recovered from the rocks of the central uplift. In this case, the impact structure resulted in a structural trap but, unlike Ames, it is not responsible for the source of the oil. Red Wing Creek is a complex structure, approximately 9 km in diameter, with seismic records and drill-core data indicating a central peak in which strata have been uplifted by up to 1 km, an annular trough containing

crater-fill products, and a partially eroded structural rim (Brenan *et al.* 1975; Sawatsky 1977). As the result of a pronounced seismic anomaly, Shell Oil drilled the structure in 1965 on the NW flank of the central uplift. The drill hole indicated a structurally high and thickened Mississippian and Pennsylvanian section, compared to drill holes outside the structure. The well, however, was dry. In 1968, Shell drilled another hole to the NW in the annular trough. Here, the Mississippian was found to be structurally low compared to exterior. It was also dry and the structure, as a whole, was assumed to be dry. True Oil redrilled what was later recognized as the central uplift in 1972 and discovered *c.* 820 m of Mississippian oil column, with considerable high angle structural complexity and brecciation and a net pay of approximately 490 m. This is in contrast to the area outside the structure, which displays gentle dips and *c.* 30 m oil columns.

The large oil column is due to the structural repetition of the Mississippian Mission Canyon Formation in the central uplift (Brenan *et al.* 1975). The impact-induced porosity and permeability results in relatively high flow rates of more than 1000 barrels per day. Cumulative production in the 20 years since discovery is in excess of 12.7 million barrels of oil and 16.2 billion cubic feet of natural gas (Pickard 1994). Current production is restricted to about 300 000 barrels per year, to preserve unexploited reserves of natural gas. However, it is estimated that the brecciated central uplift contains more than 120 million barrels of oil and primary and secondary recoverable reserves may exceed 70 million barrels (Donofrio 1981, 1998; Pickard 1994). The natural gas reserves are estimated at 100 billion cubic feet. Virtually all the oil has been discovered within a diameter of 3 km, corresponding to the central uplift. Based on net pay and its limited aerial extent, Red Wing is the most prolific oil field in the United States, in terms of producing wells per area, with the wells in the central uplift having the highest cumulative productivity of all the wells in North Dakota.

The Avak structure is located on the Arctic coastal plain of Alaska, USA. The structure has been known for some time as a 'disturbed zone' in seismic data (Lantz 1981) and hydrocarbons were discovered in 1949 (Donofrio 1998). Only recently was evidence of shock metamorphism discovered in the form of shatter cones and planar deformation features in quartz (Kirschner *et al.* 1992). The structure itself has the form of a complex impact structure roughly 12 km in diameter. It is bounded by listric faults, which define a rim area, and has an annular trough and central uplift. In the central uplift, the Lower–Middle Jurassic Kingak Shale and Barrow sand are uplifted more than 500 m from their regional levels. The central uplift has been penetrated by the Avak 1 well, which penetrated to a depth of 1225 m. Oil shows occur in Avak 1 but the well is not a commercial producer. Kirschner *et al.* (1992) suggest that pre-Avak hydrocarbon accumulations may have been disrupted and lost due to the formation of the Avak structure. There are, however, the South Barrow, East Barrow and Sikulik gas fields, which are post-impact and are related to the Avak structure. They occur outside the structure and are due to listric faults in the crater rim, which have truncated the Lower Jurassic Barrow sand and placed Lower Cretaceous Torok shales against the sand, creating an effective up-dip gas seal. The South and East Barrow fields are currently in production and primary recoverable gas is estimated at 37 billion cubic feet (Lantz 1981).

The Campeche Bank in the SE corner of the Gulf of Mexico is the most productive hydrocarbon producing area in Mexico. Oil and gas, from Jurassic source rocks, are recovered from breccia deposits at the Cretaceous–Tertiary (K/T) boundary. This area includes the world-class Cantarell oil field (Santiago-Acevedo 1980), which has produced close to 7 billion barrels of oil and 3 trillion cubic feet of gas, since discovery in 1974 to 1999. The bulk of production comes from the breccias at the K/T boundary. Primary reserves may range as high as 30 billion barrels of oil and 15 trillion cubic feet of gas. Production from the K/T boundary rocks is from up to 300 m of dolomitized limestone breccia, with a porosity of around 10%. Clasts of shocked quartz and plagioclase occur in the upper portion of the K/T breccia (Limon *et al.* 1994; Grajales-Nishimura *et al.* 2000). These breccias are the reservoir rocks for the hydrocarbons. The traps are Tertiary structural traps in the form of faulting and anticlinal structures. The seal to the reservoir rocks is an impermeable bentonitic bed, several tens of metres thick, which contains fragments of quartz and plagioclase with PDFs and some pristine impact melt glass fragments (Grajales-Nishimura *et al.* 2000). This bentonitic bed, with shocked materials, is considered to be altered ejecta materials from the K/T impact structure Chicxulub, which lies some 350 to 600 km to the NE.

Grajales-Nishimura *et al.* (2000) proposed the following sequence of events from the K/T lithologies. The main, hydrocarbon-bearing, breccias resulted from the collapse of the

offshore carbonate platform resulting from seismic energy from the Chicxulub impact. This was followed by the deposition of K/T ejecta through slower atmospheric transport. The upper part of the ejecta deposit was later reworked by the action of impact-related tsunamis crossing the Gulf of Mexico. Subsequent dolomitization and Tertiary tectonics served to form the seal and trap for migrating Jurassic hydrocarbons, resulting in an oil field that produces more than 60% of Mexico's daily production and has reserves in excess of the entire onshore and offshore hydrocarbon reserves of the United States, including Alaska (Donofrio 1998). This oil field also accounts for the bulk of the current US$16 billion gross value of hydrocarbons produced from North American impact structures per year.

Other impact structures also produce hydrocarbons. For example, the 25 km diameter Steen River structure, Canada, produces oil from two wells on the northern rim. Oil and gas are produced from beneath the *c.* 13 km diameter Marquez and Sierra Madera structures, USA (Donofrio 1997, 1998). Newporte, which was noted earlier (Clement & Mayhew 1979), and Viewfield, Canada (Sawatsky 1977) also produce hydrocarbons. These are simple bowl-shaped craters. Viewfield has approximately 50 wells (Fig. 20) producing some 600 barrels of oil and 250 million cubic feet of gas per day. The recoverable reserves associated with Viewfield are estimated to be 10–20 million barrels of oil (Donofrio 1997, 1998). More than 500 000 barrels of oil have been produced since 1978 from the Calvin structure, USA, which is most likely an 8.5 km diameter complex impact structure (Milstein 1988).

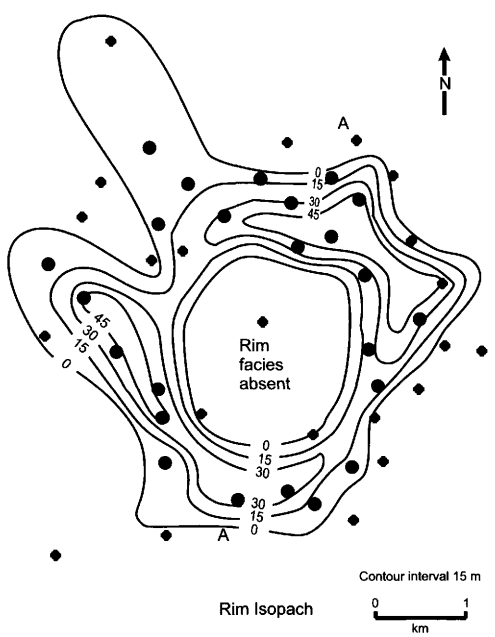

Fig. 20. Thickness of rim facies at Viewfield impact structure (Table 2). Black dots are hydrocarbon producing wells. Black dots with crosses are service or dry wells. Modified from Sawatzky (1977).

Oil shales are known at Boltysh (25 km, 88 ± 3 Ma), Obolon (15 km, 215 ± 25 Ma) and Rotmistrovka (2.7 km, 140 ± 20 Ma) in the Ukraine (Masaitis *et al.* 1980; Gurov & Gurova 1991). They represent the unmatured equivalent of the hydrocarbon reserves at Ames. The most significant reserves are at Boltysh, where there are an estimated 4.5 billion tonnes (Bass *et al.* 1967). The oil shales are the result of biological activity involving algae in this isolated basin.

Concluding remarks

The total gross direct worth of natural resources from impact structures in North America alone is estimated at in excess of US$18 billion per year. Given the relatively small number of known impact structures, as a class of geological features, impact structures have considerable overall economic potential. There are areas of the world where the numbers of known impact structures are well below those expected from the known cratering rate, indicating that there are impact structures yet to be found. For example, the average cratering rate suggests that approximately 17 ± 8 structures with diameter of 20 km or more should have been formed in an area the size of Africa (approximately 30×10^6 km^2) in the last 100 Ma. The known impact record in Africa indicates no impact structures of the appropriate size and age. However, the *c.* 80 km diameter 145 Ma Morokweng impact structure in South Africa has approximately 500 ppm Ni in its impact-melt rocks. The nickel and other PGEs occur as Ni-oxides, Ni-sulphides and as high Ni content in silicates, e.g. 0.2% NiO in orthopyroxene (Hart *et al.* 2002; Koeberl & Reimold 2003). Unlike Sudbury, the metals appear to have come from the impacting body, which was an ordinary chondrite (McDonald *et al.* 2001). Although high Ni and PGE concentrations have been found in drill core associated with thin zones containing highly altered projectile fragments (Hart *et al.* 2002), the available evidence suggests that the impact melt failed to produce immiscible sulphides and, thus, large concentrations of metals in ore deposits.

The largest impact structures have the

greatest probability of having significant economic resources. These are the most energetic events; they affect the largest volumes of target rocks, have the largest post-impact hydrothermal systems and form the largest topographic basins. It is estimated that ten impact structures in the size range of Sudbury were formed on the Earth's land surface in the last 2 Ga. At present three are known: Chicxulub, Sudbury and Vredefort. Chicxulub is buried beneath 1 km of post-impact sediments and is unlikely, therefore, to have economically viable mineral deposits; although, it has exerted considerable control over the local hydrology (Perry *et al.* 2002) and resulted in a world-class oil field at Campeche. Both Sudbury and Vredefort are major mining camps, with world-class syngenetic and progenetic ore deposits, respectively.

Impact structures do have a general property that is an advantage in the exploration for natural resources. They have relatively fixed morphometric and structural relationships for a given diameter. Once a structure is known to be of impact origin, and its diameter established, it is possible to make considerable predictions as to the structural and lithological character of the structure as a whole. This scale-depending characteristic is generally lacking in most endogenic geological structures. The development of an exploration strategy based on these relationships is most notably illustrated, in hindsight, by the drilling for hydrocarbons at Ames. Similarly, one can only speculate how the level of current knowledge on the origin and evolution of Sudbury as an impact structure will guide future mineral exploration there.

For progenetic types of deposits, the central uplift area and annular trough of complex impact structures are the most promising targets. They result in environments where buried ore deposits are structurally brought close to the surface or near surface deposits are down-dropped and protected from erosion. Syngenetic deposits are less associated with the physical redistribution of lithologies and structural changes and more closely associated with the effects of shock metamorphism through phase changes. They are, thus, more likely to be concentrated in and around such lithologies as impact melt sheets and suevitic breccias. Secondary syngenetic associations are also to be expected due to hydrothermal processes in areas above and below such lithologies. Epigenetic deposits are most closely linked with the crater form itself; generally as an isolated basin with localized sedimentary and geochemical activity not present in the area or as a set of structures controlling the migration of fluids. The brecciated and fractured rocks of the central uplift also provide an environment for the structural repetition of beds and increased porosity and permeability and are targets for hydrocarbon exploration.

Reviews of the manuscript by R. Davies, W.U. Reimold and A. Therriault are appreciated. Geological Survey of Canada Contribution 2004024.

References

ABRAMOV, O. & KRING, D.A. 2004. Numerical modeling of an impact-induced hydrothermal system at the Sudbury crater. *Journal of Geophysical Research*, **109**, E10007; doi: 10.1029/2003JE002213.

AMES, D.E., WATKINSON, D.H. & PARRISH, R.R. 1998. Dating of a regional hydrothermal system induced by the 1850 Ma Sudbury impact event. *Geology*, **26**, 447–450.

AMES, D.E., JONASSON, I.R., GIBSON, H.L. & POPE, K.O. 2005. Impact-generated hydrothermal system from the large Paleoproterozoic Sudbury crater, Canada. *In*: COCKELL, C., GILMOUR, I. & KOEBERL, C. (eds) *Biological Processes associated with Impact Events*. Impact Studies, Springer-Verlag, Berlin-Heidelberg (in press).

ARISKIN, A.A., DEUTSCH, A. & OSTERMANN, M. 1999. The Sudbury 'Igneous' Complex: Simulating phase equilibria and *in situ* differentiation for two proposed parental magmas. *In*: DRESLER, B.O. & SHARPTON, V.L. (eds) *Large Meteorite Impacts and Planetary Evolution II*. Geological Society of America Special Paper, **338**, 373–387.

BARNICOAT, A.C., YARDLEY, B.W.D., HENDERSON, I.H.C. & FOX, N.P.C. 1999. Discussion of detrital origin of hydrothermal gold by H.E. Frimmel. *Terra Nova*, **10**, 347–349.

BASS, YU. B., GALAKA, A.I. & GRABOVSKIY, V.I. 1967. [The Boltysh oil shales.] *Razvadka I Okhrana Nedr*, **9**, 11–15 [in Russian].

BAUDEMONT, D. & FEDOROWICH, J. 1996. Structural control of uranium mineralization at the Dominique Peter deposit, Saskatchewan, Canada. *Economic Geology*, **91**, 855–874.

BELL, K., CACCIOTTI, A.D. & SCHNESSL, J.H. 1985. Petrography and geochemistry of the Earl River Complex, Carswell structure, Saskatchewan – a possible Proterozoic komatiitic succession. *Geological Association Canada Special Paper*, **29**, 71–80.

BOERNER, D.E., MILKEREIT, B. & DAVIDSON, A. 1999. Geoscience impact: A synthesis of studies of the Sudbury Structure. *Canadian Journal of Earth Sciences*, **37**, 477–501.

BRENAN, R.L., PETERSON, B.L. & SMITH, H.J. 1975. The origin of Red Wing Creek Structure, McKenzie County, North Dakota. *Wyoming Geological Association Earth Science Bulletin*, **8**, 1–41.

CARPENTER, B.N. & CARLSON, R. 1992. The Ames impact crater. *Oklahoma Geological Survey*, **52**, 208–223.

CARPENTER, B.N. & CARLSON, R. 1997. The Ames meteorite impact crater. *In*: JOHNSON, K.S. & CAMPBELL, J.A. (eds) *Ames structure in northwest Oklahoma and similar features: Origin and petroleum production (1995 Symposium)*. Oklahoma Geological Survey Circular, **100**, 104–119.

CARTER, N.L. 1965. Basal quartz deformation lamellae – a criterion for recognition of impactites. *American Journal Science*, **263**, 786–806.

CARTER, W.M., WATKINSON, D.H. & JONES, P.C. 2001. Post-magmatic remobilisation of platinum-group elements in the Kelly Lake Cu–Ni sulfide deposit, Copper Cliff Offset, Sudbury. *Exploration Mining Geology*, **10**, 95–110.

CHAO, E.C.T., FAHEY, J.J., LITTLER, J. & MILTON, D.J. 1962. Stishovite, SiO_2, a very high pressure new mineral from Meteor Crater, Arizona. *Journal of Geophysical Research*, **67**, 419–421.

CLEMENT, J.H. & MAYHEW, T.E. 1979. Newporte discovery opens new pay. *Oil & Gas Journal*, **77**, 165–172.

COHEN, A.S., BURNHAM, O.M., HAWKESWORTH, C.J. & LIGHTFOOT, P.C. 2000. Pre-emplacement Re–Os ages for utramafic inclusions in the sublayer of the Sudbury Igneous Complex, Ontario. *Chemical Geology*, **165**, 37–46.

COLLINS, W.H. 1934. Life-history of the Sudbury Nickel Irruptive, Part I, Petrogenesis. *Transactions of the Royal Society of Canada*, **28**, 123–177.

CORFU, F. & LIGHTFOOT, P.C. 1996. U-Pb geochronology of the sublayer environment, Sudbury Igneous Complex, Ontario. *Economic Geology*, **91**, 1263–1269.

COWAN, E.J. & SCHWERDTNER, W.M. 1994. Fold origin of the Sudbury Basin. *In*: LIGHTFOOT, P.C. & NALDRETT, A.J. (eds) *Proceedings of the Sudbury –Noril'sk Symposium*, Ontario Geological Survey Special Volume, **5**. Toronto, Ministry of Northern Development and Mines, 45–55.

CURRIE, K.L. 1969. Geological notes on the Carswell circular structure, Saskatchewan (74K). *Canadian Geological Survey of Canada Paper*, **67-32**, 1–60.

CURTISS, D.K. & WAVREK, D.A. 1997. The Oil Creek–Arbuckle Petroleum System, Major county, Oklahoma. *In*: JOHNSON, K.S. & CAMPBELL, J.A. (eds) *Ames structure in northwest Oklahoma and similar features: Origin and petroleum production (1995 Symposium)*. Oklahoma Geological Survey Circular, **100**, 240–258.

CYMBAL, S.N. & POLKANOV, YU. A. 1975. [*Mineralogy of titanium-zirconium placers of Ukraine.*] Nauk Press, Kiev [in Russian].

DENCE, M.R. 1972. The nature and significance of terrestrial impact structures. *24th International Geological Congress Section*, **15**, 77–89.

DEUTSCH, A. & GRIEVE, R.A.F. 1994. The Sudbury Structure: Constraints on its genesis from the probe results. *Geopyhsics Research Letters*, **21**, 963–966.

DICKIN, A.P., RICHARDSON, J.M., CROCKET, J.H., MCNUTT, R.H. & PEREDERY, W.V. 1992. Osmium isotope evidence for a crustal origin of platinum group elements in the Sudbury nickel ore, Ontario, Canada. *Geochimica et Cosmochimica Acta*, **56**, 3531–3537.

DICKIN, A.P., ARTAN, M.A. & CROCKET, J.H. 1996. Isotopic evidence for distinct crustal sources of North and South Range ores, Sudbury Igneous Complex. *Geochimica et Cosmochimica Acta*, **60**, 1605–1613.

DICKIN, A.P., NGUYEN, T. & CROCKET, J.H. 1999. Isotopic evidence for a single impact melting origin of the Sudbury Igneous Complex. *In*: DRESSLER, B.O. & SHARPTON, V.L. (eds) *Large Meteorite Impacts and Planetary Evolution II*. Geological Society of America Special Paper, **339**, 361–371.

DIETZ, R.S. 1961. Vredefort ring structure. Meteorite impact scar? *Journal of Geology*, **69**, 499–516.

DIETZ, R.S. 1968. Shatter cones in cryptoexplosion structures. *In*: FRENCH, B.M. & SHORT, N.M. (eds) *Shock Metamorphism of Natural Materials*. Mono Book Corporation, Baltimore, 267–285.

DONOFRIO, R.R. 1981. Impact craters: Implications for basement hydrocarbon production. *Journal of Petroleum Geology*, **3**, 279–302.

DONOFRIO, R.R. 1997. Survey of hydrocarbon-producing impact structures in North America: Exploration results to date and potential for discovery in Precambrian basement rock. *In*: JOHNSON, K.S. & CAMPBELL, J.A. (eds) *Ames Structure in Northwest Oklahoma and Similar Features: Origin and Petroleum Production (1995 Symposium)*. Oklahoma Geological Survey Circular, **100**, 17–29.

DONOFRIO, R.R. 1998. North American impact structures hold giant field potential. *Oil & Gas Journal*, **May**, 69–83.

DRESSLER, B.O. 1984*a*. General geology of the Sudbury area. *In*: PYE, E.G., NALDRETT, A.J. & GIBLIN, P.E. (eds) *The Geology and Ore Deposits of the Sudbury Structure*. Ministry of Natural Resources, Toronto, 57–82.

DRESSLER, B.O. 1984*b*. The effects of the Sudbury event and the intrusion of the Sudbury igneous complex on the footwall rocks of the Sudbury Structure. *In*: PYE, E.G., NALDRETT, A.J. & GIBLIN, P.E. (eds) *The Geology and Ore Deposits of the Sudbury Structure*. Ministry of Natural Resources, Toronto, 97–136.

ENGELHARDT, W.V. 1990. Distribution, petrography and shock metamorphism of the ejecta of the Ries crater in Germany – a review. *Tectonophysics*, **171**, 259–273.

EZERSKII, V.A. 1982. [Impact-metamorphosed carbonaceous matter in impactites.] *Meteoritika*, **41**, 134–140 [in Russian].

FAGGART, B.E. JR., BASU, A.R. & TATSUMOTO, M. 1985. Origin of the Sudbury complex by meteoritic impact: Neodymium isotopic evidence. *Science*, **230**, 436–439.

FARLEY, K.A. 2001. Extraterrestrial helium in seafloor sediments: Identification, characteristics and accretion rate over geologic time. *In*: PEUCKER-EHRENBRINK, B. & SCHMITZ, B. (eds) *Accretion of extraterrestrial matter throughout Earth's history*. Kluwer Academic/Plenum Publishers, New York, 179–204.

FARROW, C.E.G. & LIGHTFOOT, P.C. 2002. Sudbury

PGE revisited: Toward an integrated model. *In*: CABRI, L.J. (ed.) *The geology, geochemistry, mineralogy and beneficiation of platinum-group elements*. Canadian Institute of Mining and Metallurgy Special Volume, **54**, 273–297.

FARROW, C.E.G. & WATKINSON, G.H. 1997. Diversity of precious-metal mineralization in footwall Cu–Ni–PGE deposits, Sudbury, Ontario. Implications for hydrothermal models of formation. *Canadian Mineralogist*, **35**, 817–839.

FRENCH, B.M. 1998. *Traces of a Catastrophe: A Handbook of Shock Metamorphic Effects in Terrestrial Meteorite Impact Structures*. LPI Contribution, **No. 954**, Lunar and Planetary Institute, Houston TX.

FRIMMEL, H.E., HALLBAUER, D.K. & GARTZ, V.H. 1999. Gold mobilizing fluids in the Witwatersrand Basin: Composition and possible sources. *Mineralogy and Petrology*, **66**, 55–81.

GIBBINS, W.A. & MCNUTT, R.H. 1975. The age of the Sudbury Nickel Irruptive and the Murray granite. *Canadian Journal Earth Sciences*, **12**, 1970–1989.

GIBLIN, P.E. 1984*a*. History of exploration and development, of geological studies and development of geological concepts. *In*: PYE, E.G., NALDRETT, A.J. & GIBLIN, P.E. (eds) *The Geology and Ore Deposits of the Sudbury Structure*. Ministry of Natural Resources, Toronto, 3–23.

GIBLIN, P.E. 1984*b*. Glossary of Sudbury geology terms. *In*: PYE, E.G., NALDRETT, A.J. & GIBLIN, P.E. (eds) *The Geology and Ore Deposits of the Sudbury Structure*. Ministry of Natural Resources, Toronto, 571–574.

GIBSON, R.L. & REIMOLD, W.V. 1999. The significance of the Vredefort Dome for the thermal and structural evolution of the Wiwatersrand Basin, South Africa. *Mineralogy and Petrology*, **66**, 5–23.

GIBSON, R.L. & REIMOLD, W.V. 2000. Deeply exhumed impact structures; a case study of the Vredefort Structure, South Africa. *In*: GILMOUR, I. & KOEBERL, C. (eds) *Impacts and the early Earth*. Lecture Notes in Earth Science, **91**, 249–277.

GIBSON, R.L., REIMOLD, W.V. & STEVENS, G. 1998. Thermal–metamorphic signature of an impact event in the Vredefort Dome, South Africa. *Geology*, **26**, 787–790.

GRAJALES-NISHIMURA, J.M., CEDILLO-PARDO, E., ROSALES-DOMINGUEZ, C., *ET AL.* 2000. Chicxulub impact. The origin of reservoir and seal facies en the southeastern Mexico oil fields. *Geology*, **28**, 307–310.

GRANT, R.W. & BITE, A. 1984. Sudbury quartz diorite offset dikes. *In*: PYE, E.G., NALDRETT, A.J. & GIBLIN, P.E. (eds) *The Geology and Ore Deposits of the Sudbury Structure*. Ministry of Natural Resources, Toronto, 275–300.

GRIEVE, R.A.F. & FLORAN, R.J. 1978. Manicouagan impact melt, Quebec. II: Chemical interrelations with basement and formational processes. *Journal of Geophysical Research*, **83**, 2761–2771.

GRIEVE, R.A.F. & MASAITIS, V.L. 1994. The economic potential of terrestrial impact craters. *International Geology Review*, **36**, 105–151.

GRIEVE, R.A.F. & PILKINGTON, M. 1996. The signature of terrestrial impacts. *AGSO Journal of Australian Geology and Geophysics*, **16**, 399–420.

GRIEVE, R.A.F. & THERRIAULT, A.M. 2000. Vredefort, Sudbury, Chicxulub: Three of a kind? *Annual Review of Earth & Planetary Sciences*, **28**, 305–338.

GRIEVE, R.A.F. & THERRIAULT A.M. 2004. Observations at terrestrial impact structures: Their utility in constraining crater formation. *Meteorites and Planetary Science*, **39**, 199–216.

GRIEVE, R.A.F., CODERRE, J.M., ROBERTSON, P.B. & ALEXOPOULOS, J.S. 1990. Microscopic planar deformation features in quartz of the Vredefort structure: Anomalous but still suggestive of an impact origin. *Tectonophysics*, **171**, 185–200.

GRIEVE, R.A.F., STÖFFLER, D. & DEUTSCH, A. 1991. The Sudbury Structure: Controversial or misunderstood? *Journal of Geopyhsical Research*, **96**, 22 753–22 764.

GRIEVE, R.A.F., LANGENHORST, F. & STÖFFLER, D. 1996. Shock metamorphism of quartz in nature and experiment: II. Significance in geoscience. *Meteoritics and Planetary Science*, **31**, 6–35.

GUROV, E.P. & GUROVA, E.P. 1991. [*Geological structure and composition of rocks in impact craters.*] Nauk Press, Kiev [in Russian].

GUROV, E.P., MELNYCHUK, E.V., METALIDI, S.V., RYABENKO, V.A. & GUROVA, E.P. 1985. [The characteristics of the geological structure of the eroded astrobleme in the western part of the Ukranian Shield.] Dopovidi Akad. *Nauk Ukrainskoi Radyanskoi Sotsialisychnoi Respubliky*, **Seriya B**, 8–11 [in Ukrainian].

GUROV, E.P., GUROVA, E.P. & RATISKAYA, R.B. 1996. Impact diamonds of the Zapadnaya crater; phase composition and some properties (abstract). *Meteroritics & Planetary Science*, **31 Supplement**, 56.

HARGRAVES, R.B. 1961. Shatter cones in the rocks of the Vredefort Ring. *Transactions and Proceedings Geological Society of South Africa*, **64**, 147–154.

HART, R.J., CLOETE, M., MCDONALD, I., CARLSON, R.W. & ANDREOLI, M.A.G. 2002. Siderophile-rich inclusions from the Morokweng impact melt sheet, South Africa: possible fragments of a chondritic meteorite. *Earth and Planetary Science Letters*, **198**, 49–62.

HARPER, C.T. 1982. Geology of the Carswell structure, central part. *Saskatchewan Geological Survey, Report*, **214**, 1–6.

HENKEL, H. 1992. Geophysical aspects of meteorite impact craters in eroded shield environment, with special emphasis on electric resistivity. *Tectonophysics*, **216**, 63–90.

HENKEL, H. & REIMOLD, W.U. 1998. Integrated geophysical modelling of a giant, complex impact structure: Anatomy of the Vredefort Structure, South Africa. *Tectonophysics*, **287**, 1–20.

HILDEBRAND, A.R., CAMARGO, A.Z., JACOBSEN, S.B., BOYNTON, W.V., KRING, D.A., PENFIELD, G.T. & PILKINGTON, M. 1991. Chicxulub crater: A possible Cretaceous–Tertiary boundary impact crater on the Yucatan Peninsula, Mexico. *Geology*, **19**, 867–871.

HIRT, A.M., LOWRIE, W., CLENDENEN, W.S. & KLIGFIELD, R. 1993. Correlation of strain and the anisotropy of magnetic susceptibility in the Onaping Formation: Evidence for a near-circular origin of the Sudbury Basin. *Tectonophysics*, **225**, 231–254.

HÖRZ, F. 1968. Statistical measurements of deformation structures and refractive indices in experimentally shock loaded quartz. *In*: FRENCH, B.M. & SHORT, N.M. (eds) *Shock Metamorphism of Natural Materials*. Mono Book Corporation, Baltimore, 243–253.

HOUGH, R.M., GILMOUR, I., PILLIGER, C.T., ARDEN, J.W., GILDES, K.W.R., YUAN, J. & MILLEDGE, H.J. 1995. Diamond and silicon carbide in impact melt rock from the Ries impact crater. *Nature*, **378**, 41–44.

HURST, R.W. & FARHAT, J. 1977. Geochronologic investigations of the Sudbury nickel irruptive and the Superior Province granites north of Sudbury. *Geochimica et Cosmochimica Acta*, **41**, 1803–1815.

INNES, M.J.S. 1964. Recent advances in meteorite crater research at the Dominion Observatory, Ottawa, Canada. *Meteoritics*, **2**, 219–241.

JAHN, B., FLORAN, R.J. & SIMONDS, C.H. 1978. Rb–Sr isochron age of the Manicouagan melt sheet, Quebec, Canada. *Journal of Geophysical Research*, **83**, 2799–2803.

JAMES, R.S., PEREDERY, W. & SWEENY, J.M. 1992. Thermobarometric studies on the Levack gneisses – footwall rocks to the Sudbury Igneous Complex (abstract). International Conference on Large Meteorite Impacts & Planetary Evolution. *LPI Contribution No.* **790**, 41.

JOHNSON, K.S. & CAMPBELL, J.A. (eds) 1997. *Ames structure in northwest Oklahoma and similar features: Origin and petroleum production (1995 Symposium)*. Oklahoma Geological Survey Circular, **100**.

KETTRUP, B., AGRINIER, P., DEUTSCH, A. & OSTERMANN, M. 2000. Chicxulub impactites: Geochemical clues to precursor rocks. *Meteoritics and Planetary Science*, **35**, 1129–1158.

KETTRUP, B., DEUTSCH, A. & MASAITIS, V.L. 2003. Homogeneous impact melts produced by a heterogeneous target? Sr–Nd isotopic evidence from the Popigai crater, Russia. *Geochimica et Cosmochimica Acta*, **67**, 733–750.

KIEFFER, S.W. 1971. Shock metamorphism of the Coconino sandstone at Meteor Crater, Arizona. *Journal of Geophysical Research*, **76**, 5449–5473.

KIRSCHNER, C.E., GRANTZ, A. & MULLEN, W.W. 1992. Impact origin of the Avak Structure and genesis of the Barrow gas fields. *American Association of Petroleum Geologists Bulletin*, **76**, 651–679.

KOEBERL, C. & REIMOLD, W.U. 2003. Geochemistry and petrography of impact breccias and target rocks from the 145 Ma Morokweng impact structure, South Africa. *Geochimica et Cosmochimica Acta*, **67**, 1837–1862.

KOEBERL, C. & SHIREY, S.B. 1997. Re–Os isotope systematics as a diagnostic tool for the study of impact craters and ejecta. *Paleogeography, Paleoclimatology, Paleoecology*, **132**, 25–46.

KOEBERL, C., REIMOLD, W.U., SHIREY, S.B. & LE ROUX, F.G. 1994. Kalkkop crater, Cape Province, South Africa: Confirmation of impact origin using osmium isotope systematics. *Geochimica et Cosmochimica Acta*, **58**, 1229–1234.

KROCHUK, R.V. & SHARPTON, V.L. 2002. Overview of Terny astrobleme (Ukranian Shield) studies (abstract). *Lunar and Planetary Science*, **XXXIII**, 1832 pdf.

KROCHUK, R.V. & SHARPTON, V.L. 2003. Morphology of the Terny astrobleme based on field observations and sample analysis (abstract). *Lunar and Planetary Science*, **XXXIV**, 1489 pdf.

KROGH, T.E., DAVIS, D.W. & CORFU, F. 1984. Precise U–Pb zircon and baddeleyite ages for the Sudbury area. *In*: PYE, E.G., NALDRETT, A.J. & GIBLIN, P.E. (eds) *The Geology and Ore Deposits of the Sudbury Structure*. Ontario Ministry of Natural Resources, Toronto, 431–446.

KUO, H.Y. & CROCKETT, T.H. 1979. Rare earth elements in the Sudbury nickel irruptive: Comparison with layered gabbros and implications for nickel irruptive petrogenesis. *Economic Geology*, **74**, 590–605.

KUYKENDALL, M.D., JOHNSON, C.L. & CARLSON, R.A. 1997. Reservoir characterization of a complex impact structure: Ames impact structure, northern shelf, Anadarko basin. *In*: JOHNSON, K.S. & CAMPBELL, J.A. (eds) *Ames structure in northwest Oklahoma and similar features: Origin and petroleum production (1995 Symposium)*. Oklahoma Geological Survey Circular, **100**, 199–206.

LAINÉ, R.T. 1986. Uranium deposits of Carswell structure. *In*: EVANS, E.L. (ed.) *Uranium Deposits of Canada*. Canadian Institute of Mining and Metallurgy Special Volume, **33**, 155–169.

LAINÉ, R., ALONSO, D. & SVAB, M. (eds) 1985. *The Carswell Structure Uranium Deposits, Saskatchewan*. Geological Association of Canada Special Paper, **29**.

LANGENHORST, F. 2002. Shock metamorphism of some minerals: Basic introduction and microstructural observations. *Bulletin Czech Geological Survey*, **77**, 265–282.

LANGENHORST, F. & DEUTSCH, A. 1994. Shock experiments on pre-heated α and β-quartz: I. Optical and density data. *Earth and Planetary Science Letters*, **125**, 407–420.

LANGENHORST, F., SHAFRANOVSKY, G. & MASAITIS, V.L. 1998. A comparative study of impact diamonds from the Popigai, Ries, Sudbury and Lappajärvi craters (abstract). *Meteoritics and Planetary Science*, **33 Supplement**, 90–91.

LANTZ, R. 1981. Barrow gas fields – N. Slope, Alaska. *Oil & Gas Journal*, **79**, 197–200.

LESHER, C.M & THURSTON, P.C. (eds) 2002. A special issue devoted to mineral deposits of the Sudbury Basin. *Economic Geology*, **97**, 1373–1606.

LIGHTFOOT, P.C. & FARROW, C.E.G. 2002. Geology, geochemistry and mineralogy of the Worthington offset dike: A genetic model for offset dike mineralization in the Sudbury Igneous Complex. *Economic Geology*, **97**, 1419–1446.

LIMON, M., CEDILLO, E., QUEZADA, J.M., *ET AL.* 1994. Cretaceous-Tertiary boundary sedimentary breccias from southern Mexico: Normal sedimentary deposits or impact-related breccias? (abstract). *AAPG Annual Convention*, 199.

MAGYAROSI, Z., WATKINSON, D.H. & JONES, P.C. 2002. Mineralogy of Ni–Cu–Platinum Group Element sulfide ore in the 800 and 810 ore bodies, Copper Cliff South Mine, and *P-T-X* conditions during the formation of platinum-group minerals. *Economic Geology*, **97**, 147–1486.

MANTON, W.I. 1965. The orientation and origin of shatter cones in the Vredefort Ring. *New York Academy of Science Annals*, **123**, 1017–1049.

MARSHALL, D., WATKINSON, D.H., FARROW, C., MOLNAR, F. & FOUILLAC, A.M. 1999. Multiple fluid generations in the Sudbury Igneous Complex. Fluid inclusions, Ar, O, H, Rb and Sr evidence. *Chemical Geology*, **154**, 1–19.

MARTINI, J.E.J. 1978. Coesite and stishovite in the Vredefort Dome, South Africa. *Nature*, **272**, 715–717.

MARTINI, J.E.J. 1991. The nature, distribution and genesis of the coesite and stishovite associated with the pseudotachylite of the Vredefort Dome, South Africa. *Earth and Planetary Science Letters*, **103**, 285–300.

MASAITIS, V.L. 1989. The economic geology of impact craters. *International Geology Reviews*, **31**, 922–933.

MASAITIS, V.L. 1992. Impact craters: Are they useful? *Meteoritics*, **27**, 21–27.

MASAITIS, V.L. 1993. [Diamantiferous impactites, their distribution and petrogenesis.] *Regional Geology and Metallogeny*, **1**, 121–134 [in Russian].

MASAITIS, V.L. 1998. Popigai crater: Origin and distribution of diamond-bearing impactites. *Meteoritics and Planetary Science*, **33**, 349–359.

MASAITIS, V.L., DANILIN, A.I., MASHCHAK, M.S., RAIKHLIN, A.I., SELIVANOVSKAYA, T.V. & SHADENKOV, E.M. 1980. [*The Geology of Astroblemes.*] Nedra Press, Leningrad [in Russian].

MASAITIS, V.L., SHAFRANOVSKY, G.I., EZERSKY, V.A. & RESHETNYAK, N.B. 1990. [Impact diamonds from ureilites and impactites.] *Meteoritika*, **49**, 180–195 [in Russian].

MASAITIS, V.L., SHAFRANOVSKY, G.I. *ET AL.* 1999. Impact diamonds in suevite breccias of the Onaping Formation, Sudbury Structure, Ontario Canada. *In*: DRESSLER, B.O. & SHARPTON, V.L. (eds) *Large Meteorite Impacts and Planetary Evolution II.* Geological Society of America, Special Paper, **339**, 317–321.

MCCARTHY, T.S., CHARLESWORTH, E.G. & STANISTREET, I.G. 1986. Post-Transvaal structural features of the northern portion of the Witwatersrand Basin. *Transactions of the Geological Society of South Africa*, **89**, 311–323.

MCCARTHY, T.S., STANISTREET, I.G. & ROBB, L.J. 1990. Geological studies related to the origin of the Witwatersrand Basin and its mineralization: An introduction and strategy for research and exploration. *South African Journal of Geology*, **93**, 1–4.

MCCARVILLE, P. & CROSSEY, L.J. 1996. Post-impact hydrothermal alteration of the Manson impact structure. *In*: KOEBERL, C. & ANDERSON, R.R. (eds) *The Manson Impact Structure: Anatomy of an Impact Crater.* Geological Society of America Special Paper, **302**, 347–376.

MCDONALD, I., ANDREOLI, M.A.G., HART, R.J. & TREDOUX, M. 2001. Platinum-group elements in the Morokweng impact structure, South Africa: Evidence for impact of a very large ordinary chondrite projectile at the Jurassic–Cretaceous boundary. *Geochimica et Cosmochimica Acta*, **65**, 299–309.

MELOSH, H.J. 1989. *Impact Cratering: A Geologic Process.* Oxford University Press, New York.

MILKEREIT, B., GREEN, A. & SUDBURY WORKING GROUP, 1992. Deep geometry of the Sudbury structure from seismic reflection profiling. *Geology*, **20**, 807–811.

MILKEREIT, B., BOERNER, E.K., *ET AL.* 2002. Development of 3-D seismic exploration technology for deep nickel–copper deposits – A case history from the Sudbury basin, Canada. *Geophysics*, **65**, 1890–1899.

MILSTEIN, R.L. 1988. The Calvin 28 structure: Evidence for impact origin. *Canadian Journal of Earth Science*, **25**, 1524–1530.

MILTON, D.J. 1977. Shatter cones – an outstanding problem in shock mechanics. *In*: RODDY, D.J., PEPIN, R.O. & MERRILL, R.B. (eds) *Impact and Explosion Cratering.* Pergamon Press, New York, 703–714.

MINTER, W.E.L. 1999. Irrefutable detrital origin of Witwatersrand gold and evidence of eolian signatures. *Economic Geology*, **94**, 665–670.

MINTER, W.E.L., GOEDHART, M., KNIGHT, J. & FRIMMEL, H.E. 1993. Morphology of Witwatersrand gold grains from the Basal Reef: Evidence for their detrital origin. *Economic Geology*, **88**, 237–248.

MOLNAR, F., WATKINSON, D.H., JONES, P.C. & GALTER, I. 1997. Fluid inclusion evidence for hydrothermal enrichment of magmatic ore at the contact zone of Ni–Cu Platinum-group 4b deposit, Lindsley mine, Sudbury, Canada. *Economic Geology*, **92**, 674–682.

MOLNAR, F., WATKINSON, D.H. & EVEREST, J. 1999. Fluid-inclusion characteristics of hydrothermal Cu–Ni–PGE veins in granitic and metavolcanic rocks at the contact of the Little Stobie deposit, Sudbury, Canada. *Chemical Geology*, **154**, 279–301.

MOLNAR, F., WATKINSON, D.H. & JONES, P.C. 2001. Multiple hydrothermal processes in footwall units of the North Range, Sudbury Igneous Complex, Canada, and implications for the genesis of vein-type Cu–Ni–PGE deposits. *Economic Geology*, **96**, 1645–1670.

MORGAN, J., GRIEVE, R.A.F. & WARNER, M. 2002*a*. Geophysical constraints on the size and structure of the Chicxulub impact center. *In*: KOEBERL, C. & MACLEOD, K.G. (eds) *Catastrophic events and mass extinctions: Impact and beyond.* Geological Society of America Special Paper, **356**, 39–46.

MORGAN, J.W., WALKER, R.J., HORAN, M.F., BEARY, E.S. & NALDRETT, A.J. 2002*b*. ^{190}Pt-^{186}Os and ^{187}Re-^{187}Os systematics of the Sudbury Igneous Complex, Ontario. *Geochimica et Cosmochimica Acta*, **66**, 273–290.

MORRISON, G.G., JAGO, B.C. & WHITE, T.L. 1994. Footwall mineralization of the Sudbury Igneous Complex. *In*: LIGHTFOOT, P.C. & NALDRETT, A.J. (eds) *Proceedings of the Sudbury – Noril'sk Symposium*. Ontario Geological Survey Special Volume, **5**. Ministry Northern Development and Mines, Toronto, 57–64.

NALDRETT, A.J. 1984. Mineralogy and composition of the Sudbury ores. *In*: PYE, E.G., NALDRETT, A.J. & GIBLIN, P.E. (eds) *The Geology and Ore Deposits of the Sudbury Structure*. Ontario Geological Survey Special Volume, **1**. Ministry Natural Resources, Toronto, 309–325.

NALDRETT, A.J. 2003. From impact to riches: Evolution of geological understanding as seen at Sudbury, Canada. *GSA Today*, **13**, 4–9.

NALDRETT, A.J. & HEWINS, R.H. 1984. The main mass of the Sudbury Igneous Complex. *In*: PYE, E.G., NALDRETT, A.J. & GIBLIN, P.E. (eds) *The Geology and Ore Deposits of the Sudbury Structure. Ontario Geological Survey Special Volume*, **1**. Ministry Natural Resources, Toronto, 235–251.

NALDRETT, A.J. & LIGHTFOOT, P.C. 1993. *Ni–Cu–PGE ores of the Noril'sk region Siberia: A model for giant magmatic ore deposits associated with flood basalt*. Society of Economic Geologists Special Publication, **2**, 81–123.

NALDRETT, A.J., HEWINS, R.H., DRESSLER, B.O. & RAO, B.V. 1984. The contact sublayer of the Sudbury Igneous Complex. *In*: PYE, E.G., NALDRETT, A.J. & GIBLIN, P.E. (eds) *The Geology and Ore Deposits of the Sudbury Structure*. Ontario Geological Survey Special Volume, **1**. Ministry Natural Resources, Toronto, 253–274.

NAUMOV, M.V. 2002. Impact-generated hydrothermal systems: Data from Popigai, Kara and Puchezh-Katunki impact structures. *In*: PLADO, J. & PESONEN, L.J. (eds) *Impacts in Precambrian Shield*. Springer-Verlag, Berlin, 117–172.

NIKOLSKY, A.P. 1991. [*Geology of the Pervomaysk iron-ore deposit and transformation of its structure by meteoritic impact.*] Nedra Press, Moscow [in Russian].

NIKOLSKY, A.P., NAUMOV, V.P. & KOROBKO, N.I. 1981. [Pervomaysk iron deposit, Krivoj Rog and its transformations by shock metamorphism.] *Geologia rudnykh mestorozhdenii*, **5**, 92–105 [in Russian].

NIKOLSKY, A.P., NAUMOV, V.P., MASHCHAK, M.S. & MASAITIS, V.L. 1982. [Shock metamorphosed rocks and impactites of Ternorvka astrobleme.] *Transactions of VSEGEI*, **238**, 132–142 [in Russian].

ORMŐ, J., BLOMQVIST, G., STRUKELL, E.F.F. & TÖRNBERG, R. 1999. Mutually constrained geophysical data for evaluating a proposed impact structure: Lake Hummeln, Sweden. *Tectonophysics*, **311**, 155–177.

OSINSKI, G.R., SPRAY, J.G. & LEE, P. 2001. Impact-induced hydrothermal activity within Haughton impact structure, arctic Canada: Generation of a transient, warm, wet oasis. *Meteoritics and Planetary Science*, **36**, 731–745.

OSTERMANN, M., SCHÄRER, U. & DEUTSCH, A. 1996. Impact melt dikes in the Sudbury multi-ring basin (Canada): Implications from uranium–lead geochronology on the Foy Offset Dike. *Meteoritics and Planetary Science*, **31**, 494–501.

PAGEL, M. & SVAB, M. 1985. Petrographic and geochemical variations within the Carswell structure metamorphic core and their implications with respect to uranium mineralization. *Geological Association of Canada Special Paper*, **29**, 55–70.

PALME, H., GOEBEL, E. & GRIEVE, R.A.F. 1979. The distribution of volatile and siderophile elements in the impact melt of East Clearwater (Quebec). *Proceeding 10th Lunar and Planetary Science Conference*. Pergamon, New York, 2465–2492.

PALME, H., GRIEVE, R.A.F. & WOLF, R. 1981. Identification of the projectile at Brent crater, and further considerations of projectile types at terrestrial craters. *Geochimica et Cosmochimica Acta*, **45**, 2417–2424.

PATTISON, E.F. 1979. The Sudbury sublayer. *Canadian Mineralogist*, **17**, 257–274.

PERRY, E., VELAQUEZ-OLIMAN, G. & MARIN, L. 2002. The hydrogeology of the karst aquifer system of the northern Yucatan Peninsula, Mexico. *International Geology Review*, **44**, 191–221.

PEUCKER-EHRENBRINK, B. 2001. Iridium and osmium as tracers of extraterrestrial matter in marine sediments. *In*: PEUCKER-EHRENBRINK, B. & SCHMITZ, B. (eds) *Accretion of extraterrestrial matter throughout Earth's history*. Kluwer Academic/Plenum Publishers, New York. 163–178.

PHILLIPS, G.N. & LAW, J.D.M. 2000. Witwatersrand gold fields; geology, genesis and exploration. *Reviews in Economic Geology*, **13**, 459–500.

PICKARD, C.F. 1994. Twenty years of production from an impact structure, Red Wing Creek Field, McKenzie County, North Dakota. *The Contact*, **41**, 2–5.

REIMOLD, W.U., KOEBERL, C., FLETCHER, P., KILLICK, A.M. & WILSON, J.D. 1999. Pseudotachylite breccias from fault zones in the Witwatersrand Basin, South Africa: Evidence of autometasomatism and post-brecciation alteration processes. *Mineralogy and Petrology*, **66**, 25–53.

ROBERTS, C. & SANDRIDGE, B. 1992. The Ames hole. *Shale Shaker*, **42**, 118–121.

ROUSELL, D.H. 1984. Mineralization in the Whitewater group. *In*: PYE, E.G., NALDRETT, A.J. & GIBLIN, P.E. (eds) *The Geology and Ore Deposits of the Sudbury Structure*. Ontario Geological Survey Special Volume, **1**. Ministry Natural Resources, Toronto, 219–232.

SAGY, A., FINEBERG, J. & RECHES, Z. 2002. Dynamic fracture by large extra-terrestrial impacts as the origin of shatter cones. *Nature*, **418**, 310–313.

SANTIAGO-ACEVEDO, J. 1980. Giant oilfields of the Southern Zone-Mexico. *In*: HALBOUTY, M.T. (ed.) *Giant oilfield and gas fields of the decade:*

1968–1978. American Association of Petroleum Geologists Memoir, **30**, 339–385.

SAWATZKY, H.B. 1977. Buried impact craters in the Williston Basin and adjacent area. *In*: RODDY, D.J., PEPIN, R.O. & MERRILL, R.B. (eds) *Impact and Explosion Cratering*. Pergamon Press, New York, 461–480.

SCHWARZ, E.J. & BUCHAN, K.L. 1982. Uplift deduced from remanent magnetization; Sudbury area since 1250 Ma ago. *Earth and Planetary Science Letters*, **58**, 65–74.

SCOTT, R.G. & SPRAY, J.G. 2000. The South Range breccia belt of the Sudbury impact structure; a possible terrace collapse feature. *Meteoritics and Planetary Science*, **35**, 505–520.

SHARPTON, V.L., BURKE, K., *ET AL.* 1993. Chicxulub multiring impact basin: Size and other characteristics derived from gravity analysis. *Science*, **261**, 1564–1567.

SIEBENSCHOCK, M., SCHMITT, R.T. & STÖFFLER, D. 1998. Impact diamonds in glass bombs from suevite of the Ries crater, Germany (abstract). *Meteoritics and Planetary Science*, **33 Supplement**, 145.

SPRAY, J.G. & THOMPSON, L.M. 1995. Friction melt distribution in terrestrial multi-ring impact basins. *Nature*, **373**, 130–132.

SPUDIS, P.D. 1993. *The Geology of Multi-ring Impact Basins*. Cambridge University Press, Cambridge.

STÖFFLER, D. 1971. Progressive metamorphism and classification of shocked and brecciated crystalline rocks in impact craters. *Journal of Geophysical Research*, **76**, 5541–5551.

STÖFFLER, D. 1972. Deformation and transformation of rock-forming minerals by natural and experimental shock processes. I. Behavior of minerals under shock compression. *Fortschritte der Mineralogie*, **49**, 50–113.

STÖFFLER, D. 1974. Deformation and transformation of rock-forming minerals by natural and experimental shock processes. II. Physical properties of shocked minerals. *Fortschritte der Mineralogie*, **51**, 256–289.

STÖFFLER, D. 1984. Glasses formed by hypervelocity impacts. *Journal of Non-Crystalline Solids*, **7**, 465–502.

STÖFFLER, D. & HORNEMANN, U. 1972. Quartz and feldspar glasses produced by natural and experimental shock. *Meteoritics*, **7**, 371–394.

STÖFFLER, D. & LANGENHORST, F. 1994. Shock metamorphism of quartz in nature and experiment: 1. Basic observation and theory. *Meteoritics*, **29**, 155–181.

STÖFFLER, D., DEUTSCH, A., *ET AL.* 1994. The formation of the Sudbury Structure, Canada: Towards a unified impact model. *In*: DRESSLER, B.O., GRIEVE, R.A.F. & SHARPTON, V.L. (eds) Geological Society of America Special Paper, **293**, 303–318.

THERRIAULT, A.M., GRIEVE, R.A.F. & REIMOLD, W.U. 1997. Original size of the Vredefort structure: Implications for the geological evolution of the Witwatersrand Basin. *Meteoritics and Planetary Science*, **32**, 71–77.

THERRIAULT, A.M., FOWLER, A.D. & GRIEVE, R.A.F. 2002. The Sudbury Igneous Complex: A differentiated impact melt sheet. *Economic Geology*, **97**, 1521–1540.

THOMPSON, L.M., SPRAY, J.G. & KELLEY, S.P. 1998. Laser probe argon-40/argon-39 dating of pseudotachylite from the Sudbury Structure: Evidence for post impact thermal overprinting in the North Range. *Meteoritics and Planetary Science*, **33**, 1259–1269.

TONA, F., ALONSO, D. & SVAB, M. 1985. Geology and mineralization in the Carswell structure – A general approach. *Geological Association of Canada Special Paper*, **29**, 1–18.

TUCHSHERER, M.G. & SPRAY, J.G. 2002. Geology, mineralisation and emplacement of the Foy offset dike, Sudbury. *Economic Geology*, **97**, 1377–1398.

TWISS, R.S. & MOORES, E.M. 1992. *Structural Geology*. W.H. Freeman, New York.

VAL'TER, A.A., EREMENKO, G.K., KWASNITSA, V.N. & POLKANOV, YU. A. 1992. [*Shock metamorphosed carbon minerals.*] Nauk Press, Kiev [in Russian].

WALKER, R.J., MORGAN, J.W., NALDRETT, A.J., LI, C. & FASSETT, J.D. 1991. Re–Os isotope systematics of Ni–Cu sulfide ores, Sudbury Igneous Complex, Ontario: Evidence for a major crustal component. *Earth and Planetary Science Letters*, **105**, 416–429.

WARNER, S., MARTIN, R.F., ABDEL-RAHAM, A.F.M. & DOIG, R. 1998. Apatite as a monitor of fractionation, degassing and metamorphism in the Sudbury Igneous Complex, Ontario. *Canadian Mineralogist*, **36**, 981–999.

WIEST, B, 1987. *Diskordante Gangbreccien und strukturelle Merkmale im Untergrund komplexer Impaktstrukturen und ihre Bedeutung für die Kraterbildungsprozesse*. PhD thesis, Westfälische Wilhems Universität, Münster, Germany.

WOOD, C.A. & HEAD, J.W. 1976. Comparison of impact basins on Mercury, Mars and the Moon. *Proceeding 7th Lunar Science Conference*. Pergamon, New York, 3629–3651.

WU, J., MILKEREIT, B. & BOERNER, D.E. 1995. Seismic imaging of the enigmatic Sudbury structure. *Journal* of *Geophysical Research*, **100**, 4117–4130.